

**BRNO UNIVERSITY OF TECHNOLOGY
ESCUELA POLITÉCNICA DE INGENIERÍA DE GIJÓN.**

BACHELOR IN MECHANICAL ENGINEERING

*Numerical simulation of the crack propagation in
biaxial stress field*

*Simulación numérica de la propagación de grietas bajo campo biaxial de
tensiones*

D. Claudia Oliver Figueira

Supervisor: Assoc. Prof. Stanislav Seitl, Ph.D.
Supervisor specialist: Ing. Petr Miarka

May 2017.



**FAKULTA
STAVEBNÍ**



Abstract

This thesis is focused on the problematic of the prediction of the direction of the crack propagation in materials with non-linear behavior. By using different software as ANSYS (for finite element method) or Wolfram Mathematica (for numerical calculation), this document try to find the angle of crack propagation. Different approach and criteria have been used in order to compare the influence of some parameter on the crack growth (as stress intensity factor and T-stress).

Keywords

Linear elastic fracture mechanics, stress intensity factor, biaxial stress, numerical study, crack initiation, mixed mode, MTS criterion, SED criterion, CTD criterion.

Resumen

Este proyecto se basa en la problemática de la predicción de la dirección de propagación de grietas en materiales con comportamiento no lineal. Mediante el uso de diferentes programas informáticos como ANSYS (para el cálculo mediante elementos finitos) y Wolfram Mathematica (para el cálculo numérico), este documento trata de buscar la solución para el ángulo de propagación de grieta. Se han utilizado diferentes criterios para comparar la influencia de parámetros en el crecimiento de grietas (como el factor intensidad de tensiones y la tensión T)

Palabras clave

Mecánica de la fractura elástico lineal, factor intensidad de tensiones, tensiones biaxiales, estudio numérico, iniciación de grietas, modo mixto, criterio energético de fractura, abertura del frente de grieta.

Citation of this thesis

Claudia Oliver Figueira, Numerical simulation of the crack propagation in biaxial stress field, parametric study influence on angle of initiation. Brno, 2017. 62 p., Bachelor thesis. Brno University of Technology, Faculty of Civil Engineering, Institute of Structural Mechanics. Supervisor assoc. prof. Stanislav Seitl, Ph.D., Supervisor specialist Ing. Petr Miarka

This thesis is the final part of my studies in Mechanical Engineering (2011-2017) at the University of Oviedo. It has been held in Brno, Czech Republic, during Erasmus mobility in collaboration with Brno University of Technology.

I would like to thank the invaluable help of my tutors, who have made it possible for me to carry out this project, Petr Miarka, Stanislav Seitl and María Jesús Lamela Rey. Also to my family, my parents and my sister, and my fatigue collaborate Sofía. It would not have been possible without their help.

Acknowledgment

The author acknowledges the support of Czech Sciences foundation project No. 17-01589S. This thesis has been carried out under the project No. LO1408 "AdMaS UP – Advanced Materials, Structures and Technologies", supported by Ministry of Education, Youth and Sports under the „National Sustainability Programme I".

Table of content

Table of content.....	5
Table of tables	7
Table of figures.....	8
Table of graphs.....	9
1 Resumen en castellano.	10
1.1 Aclaraciones.	10
1.2 Introducción.	10
1.3 Antecedentes teóricos.	10
1.3.1 Modos de carga.....	11
1.3.2 Factor intensidad de tensiones.....	11
1.3.3 T-stress	11
1.4 Enfoques uniparamétrico y multiparamétrico.....	12
1.5 Serie de expansión de Williams.....	12
1.6 Criterios para la predicción del ángulo de propagación.	13
1.6.1 Criterio de máxima tensión tangencial. (MTS).....	13
1.6.2 Criterio de mínima densidad de energía. (SED)	14
1.6.3 Criterio de desplazamiento en la punta de grieta. (CTO).....	15
1.7 Metodología en software ANSYS.	15
1.8 Modelo numérico.....	15
1.9 Resultados.....	19
1.10 Resultados	20
1.11 Conclusiones.....	22
2 Introduction	23
3 Theoretical background	24
3.1 Loading modes	24
3.2 Stress intensity factor.....	26
3.3 T-Stress.....	28
3.4 Single-parameter and multi-parameter approach.....	29
3.5 Williams expansion.....	29
3.6 CRITERIA FOR PREDICTION OF ANGLE PROPAGATION.	30
3.6.1 Maximum tangential stress criterion (MTS criterion)	31
3.6.2 Minimum strain energy density SED CRITERIA	32
3.6.3 The CTD criterion.....	33
3.7 ANSYS METHODOLOGY	34



3.7.1	KCALC. Stress Intensity Factors in ANSYS.....	34
3.7.2	PATH command	35
4	Numerical model.....	36
4.1	Specimen geometry and dimensions	36
4.2	Coordinate systems.....	37
4.3	Element type	38
4.4	Mesh.....	39
4.5	Boundary conditions (Loads and supports)	42
4.6	Material properties	43
5	Results	44
5.1	How to get each parameter	44
5.1.1	Stress intensity factor (K_I and K_{II}).....	44
5.1.2	T-stress	49
5.1.3	Displacements (δ_I and δ_{II})	53
5.1.4	Principal Tensile Stress S_1	54
5.2	How to obtain angle of propagation θ	55
5.2.1	MTS Single-parametric approach.....	55
5.2.2	MTS Multi-parametric approach.....	58
5.2.3	Direct MTS criterion.....	59
5.2.4	SED Single-parametric approach.....	60
5.2.5	SED Multi-parametric approach.....	60
5.2.6	CTD	61
6	Discussion.....	62
7	Conclusion	69
8	Author's own work.....	70
9	References.....	71
10	Curriculum vitae	73

Table of tables

Table 1. Comparison of different criteria.....	44
Table 2. Stress Intensity Factor for different crack length ratios (I)	45
Table 3. Stress Intensity Factor for different crack length ratios (II)	46
Table 4. Stress Intensity Factor for different crack length ratios (III)	47
Table 5. Stress Intensity Factor for crack length ratio $a/W=0.5$	48
Table 6. Values of displacements in x and y direction obtained in ANSYS	53
Table 7. Values of Principal Tensile Stress for an specific geometry	54
Table 8. Values of Stress Intensity factor and T-stress for $a/W=0.1$ and crack inclination angle $\alpha=0^\circ$	58
Table 9. Values of polynomial regression a and b. Angle of propagation (Θ) calculated in means of MTS.	59
Table 10. Comparison of the angle of propagation for $a/W= 0.1$ for different criteria	64
Table 11. Comparison of the angle of propagation for $a/W= 0.2$ for different criteria	65
Table 12 Comparison of the angle of propagation for $a/W= 0.3$ for different criteria.....	66
Table 13. Comparison of the angle of propagation for $a/W= 0.4$ for different criteria	67
Table 14. Comparison of the angle of propagation for $a/W= 0.9$ for different criteria	68



Table of figures

Figure 1 Charging modes (a) mode I (or opening mode), (b) mode II (or sliding mode), (c) mode III (or tearing mode)	25
Figure 2. Bidimensional model under uniaxial load conditions	25
Figure 3. Bidimensional model under biaxial load conditions. Mixed mode (I and II).....	26
Figure 4. Crack initiation angle (θ) under mixed mode conditions.....	26
Figure 5. Squat defects in railway	26
Figure 6. Definition of the coordinate axis ahead of a crack tip. x direction is normal to the page [7]	27
Figure 7. Definition of polar coordinates with angle theta equal to zero. ($\theta = 0$) [7].....	28
Figure 8. Displacements of two coincident nodes in a loaded crack. [3].....	33
Figure 9. Path for KCALC [8]	35
Figure 10. Specimen dimension. ($B = W = 180$ mm)	36
Figure 11. Crack rotation modeling.....	37
Figure 12. Coordinate system [8].....	37
Figure 13. Polar coordinates on the model. Crack angle rotation	38
Figure 14. PLANE 183 element type on ANSYS software [8]	38
Figure 15. Distribution of keypoints and lines on right crack tip.....	39
Figure 16. Modeling of specimen. Lines.	40
Figure 17. Detail of areas on crack tip	40
Figure 18. Creating areas on geometry.....	40
Figure 19. Detail of radial mesh around crack tip	41
Figure 20 Creating model. Meshing.....	41
Figure 21 Boundary conditions for different angles (supports and loads)	42
Figure 22. Principle of action and reaction. Forces on the top and right faces. Reactions on the left and bottom faces.....	43
Figure 24. Dominant Mode II	48
Figure 25. Almost equal Mode I and II	48
Figure 26. Dominant Mode I	48
Figure 27. Path for calculation of T-stress.	49
Figure 28. σ_{xx} and σ_{yy} for a specific geometry and load case	49
Figure 29. Calculation of T-stress in Excel.....	50
Figure 30. Displacement of two coincident nodes from both faces of the crack [3].....	53
Figure 31. Path for calculation of Principal Tensile Stress	54
Figure 32. Calculation of angle of propagation (θ) in Wolfram Mathematica. MTS with T-stress approach	58
Figure 33. Calculation of angle of propagation (θ) in Wolfram Mathematica. SED with T-stress approach.	60

Table of graphs

Graph 1. to Graph 10. Evolution of T-stress for different length ratios	51-34
Graph 11. Evolution of Principal Tensile Stress and equation from results on Table 2.....	55
Graph 12. to Graph 16. Initiation angle θ for various crack angle α and ratio a/W . MTS criterion.....	56
Graph 17. to Graph 25. Comparison of influence of the stress ratio σ_1/σ_2 on initiation angle θ for various crack angle α and length ratio a/W	57
Graph 26. to Graph 46. Comparison of the angle of propagation for $a/W= 0.1$ for different criteria	64
Graph 31. to Graph 35. Comparison of the angle of propagation for $a/W= 0.2$ for different criteria	65
Graph 36. to Graph 40. Comparison of the angle of propagation for $a/W= 0.3$ for different criteria	66
Graph 41. to Graph 45. Comparison of the angle of propagation for $a/W= 0.4$ for different criteria	67
Graph 46. to Graph 50. Comparison of the angle of propagation for $a/W= 0.9$ for different criteria	68

1 Resumen en castellano.

1.1 Aclaraciones.

Las ecuaciones, las tablas y los gráficos se han numerado con el mismo número que en el documento en inglés, añadiendo un asterisco detrás del número (nº*).

Los resultados presentados en este resumen son solo una pequeña parte. Para ver más resultados y gráficos comparativos ver los apartados 5.-Results y 6.-Discussion.

1.2 Introducción.

Una de las partes más importantes en el diseño de componentes mecánicos es averiguar los fallos más comunes que provocan la fractura de los mismos. Estos fallos pueden ocurrir repentinamente en la vida de servicio de los componentes y pueden suponer riesgos y provocar accidentes.

La mecánica de la fractura clásica trata de explicar los fallos en materiales que siguen un comportamiento elástico lineal. Dado que muchos de los materiales utilizados en ingeniería no siguen este comportamiento, se tratan de buscar otras teorías aplicables a comportamientos no lineales y elástico-plásticos. Durante este proyecto se han estudiado los distintos enfoques de la mecánica de la fractura y los criterios existentes para el cálculo del ángulo de iniciación de grietas en componentes con propiedades no lineales. El cálculo de este ángulo es complejo pero es un parámetro muy importante a la hora de predecir el fallo de los componentes mecánicos. Mediante la comparación de distintos enfoques y criterios se ha buscado la solución de este ángulo.

Se ha estudiado un componente variando su geometría y condiciones de contorno para comparar los distintos resultados.

1.3 Antecedentes teóricos.

El objetivo de la mecánica de la fractura es el análisis del comportamiento mecánico en componentes agrietados. Dada la existencia de diferentes materiales es difícil predecir el fallo pero es importante predecir la velocidad y crecimiento de las grietas.

Todos los componentes mecánicos presentan defectos en su estructura cuya propagación puede ser peligrosa en su vida en servicio. Además, es difícil detectar estos defectos ya que los métodos no destructivos solo aseguran la no existencia de defectos mayores que la sensibilidad del método utilizado.

1.3.1 Modos de carga

Cualquier movimiento relativo entre las superficies de una grieta se puede obtener como combinación de tres movimientos básicos que definen los tres modos de carga. Estos pueden actuar individualmente o simultáneamente en un componente.

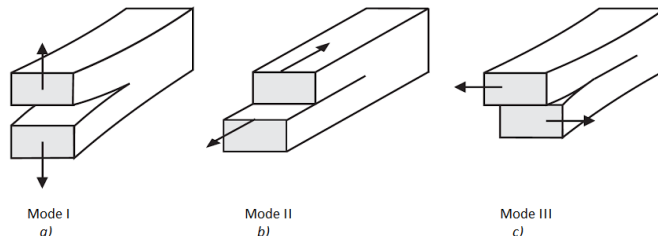


Figure 1*. Modos de carga (a) modo I, (b) modo II, (c) modo III

Los estudios de fractura han estado focalizados en el análisis del modo I, que rara vez ocurre en la práctica. El caso más general en componentes reales es la combinación de los tres modos que es muy difícil de analizar. En este documento se analizará el modo mixto como combinación de los modos I y II.

Bajo estados de cargas bidimensionales, las grietas se propagan de forma no similar, por lo que el cálculo del ángulo de iniciación de la grieta es complejo e importante a la hora de diseñar los componentes.

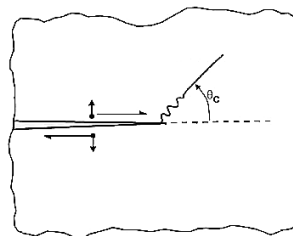


Figure 4. Crack initiation angle (θ) under mixed mode conditions.

1.3.2 Factor intensidad de tensiones.

El factor intensidad de tensiones (FIT) es uno de los parámetros más importantes de la mecánica de la fractura elástico lineal. Permite calcular el estado tensional en las proximidades de la punta de grieta. Este factor también caracteriza el modo de carga al que está sometido el componente.

1.3.3 T-stress

Otro parámetro importante es la tensión-T. En condiciones de tensión plana representa la tensión paralela a la línea de la grieta.

Generalmente, el FIT es suficiente para caracterizar el estado tensional en un componente pero existen casos donde la tensión-T puede tener un efecto importante en el campo de tensiones.

Uno de estos casos es el que ocupa este proyecto. Cuando la orientación de la grieta no es perpendicular a las cargas aplicadas y el material no sigue el comportamiento lineal, el factor *tensión-T* se utiliza para caracterizar completamente el estado tensional.

1.4 Enfoques uniparamétrico y multiparamétrico.

El enfoque tradicional de la mecánica de la fractura es la Mecánica de la Fractura Elástico Lineal (MFEL). Se trata de un enfoque uniparamétrico ya que solo tiene en cuenta el factor intensidad de tensiones para caracterizar el estado tensional de la grieta.

Sin embargo, este enfoque presenta grandes limitaciones a la hora de predecir el comportamiento de muchos materiales ya que parte de la suposición de que la zona del material con comportamiento no lineal tiene que ser pequeña en comparación con las dimensiones típicas del material. Esto solo ocurre para materiales frágiles.

Para evitar esta limitación se utiliza el llamado enfoque multiparamétrico que tiene en cuenta más parámetro que influyen en el proceso de fractura como heterogeneidades en el material, la geometría del elemento o el estado de cargas. Sus resultados son más aproximados al comportamiento real en materiales quasi-frágiles y no lineales.

1.5 Serie de expansión de Williams.

El enfoque multiparamétrico se basa en las series de expansión de Williams. La solución de Williams de los campos de tensiones y deformaciones en componentes agrietados proporciona aproximaciones razonables. Esta solución fue calculada inicialmente para materiales homogéneos, elásticos e isótropos pero el enfoque multiparamétrico consigue particularizarla para otro tipo de materiales. Su expresión es de la forma:

$$\sigma_{ij} = \sum_{n=1}^{\infty} \frac{n}{2} r^{\frac{n}{2}-1} A_n f_{ij}^{\sigma}(\theta, n) + \sum_{m=1}^{\infty} \frac{m}{2} r^{\frac{m}{2}-1} B_m g_{ij}^{\sigma}(\theta, m) \quad \mathbf{i}, \mathbf{j} \in \{\mathbf{x}, \mathbf{y}\} \quad (1^*)$$

$$u_i = \sum_{n=0}^{\infty} r^{\frac{n}{2}} A_n f_i^u(\theta, n, E, v) + \sum_{m=0}^{\infty} r^{\frac{m}{2}} B_m g_i^u(\theta, m, E, v) \quad \mathbf{i}, \mathbf{j} \in \{\mathbf{x}, \mathbf{y}\} \quad (2^*)$$

El principal propósito de este proyecto es el estudio de la influencia de la adicción de parámetros a las expresiones de Williams. Utilizando las ecuaciones anteriores y particularizándolas a la existencia de un estado de cargas biaxial (modo mixto I y II), obtenemos el campo de tensiones para componentes agrietados en los dos enfoques, clásico (utilizando solo el factor intensidad de tensiones) y multiparamétrico (añadiendo el factor *tensión-T*).

$$\sigma_{ij} = \frac{K_I}{\sqrt{2\pi r}} f_{ij}^I(\theta) + \frac{K_{II}}{\sqrt{2\pi r}} f_{ij}^{II}(\theta) \quad (3^*)$$

$$\sigma_{ij} = \frac{K_I}{\sqrt{2\pi r}} f_{ij}^I(\theta) + \frac{K_{II}}{\sqrt{2\pi r}} f_{ij}^{II}(\theta) + T \delta_{1i} \delta_{1j} \quad (4^*)$$

En ambas ecuaciones $f_{ij}(\theta)$ son funciones angulares conocidas.

1.6 Criterios para la predicción del ángulo de propagación.

A lo largo de los años se han propuesto muchos criterios para el estudio de la propagación de grietas. Muchos de ellos referidos solo a modo I, mientras que otros se pueden extrapolar al modo mixto de carga.

El criterio de la tensión tangencial máxima (MTS), Mínima densidad de Energía (SED) y Desplazamiento de la Punta de grieta (CTDO) han sido utilizados por muchos autores. En ellos, se analiza la fuerza conductor de la propagación de las grietas.

Se analizarán los diferentes criterios bajo el enfoque uniparamétrico y multiparamétrico de la mecánica de la fractura.

1.6.1 Criterio de máxima tensión tangencial. (MTS)

Es uno de los criterios más usados. Su hipótesis asume que la grieta se propagará en la dirección de la tensión tangencial máxima. La grieta comenzará en la punta de grieta y se propagará en la dirección radial donde el esfuerzo tangencial sea máximo. Matemáticamente se expresa de la forma:

$$\frac{\partial \sigma_{\theta\theta}}{\partial \theta} = 0 \quad \text{and} \quad \frac{\partial^2 \sigma_{\theta\theta}}{\partial \theta^2} < 0. \quad (5^*)$$

Combinando las expresiones del campo de tensiones en la proximidad de la grieta (expansión de Williams), con las condiciones de este criterio se obtienen las siguientes expresiones que permiten calcular el ángulo de propagación de la grieta. Se han obtenido para enfoque multi y uniparamétrico. Se puede observar que en las ecuaciones (6*) (7*) solo se tiene en cuenta el FIT mientras que en (8*) se añade la tensión- T .

Enfoque uniparamétrico.

$$K_I \sin \theta + K_{II} (3 \cos \theta - 1) = 0 \quad (6^*)$$

$$\theta = \begin{cases} 2 \operatorname{arctg} \frac{1}{4} \left(\frac{K_I}{K_{II}} + \sqrt{\left(\frac{K_I}{K_{II}} \right)^2 + 8} \right) & \text{for } K_{II} < 0 \\ 0 & \text{for } K_{II} = 0 \\ 2 \operatorname{arctg} \frac{1}{4} \left(\frac{K_I}{K_{II}} - \sqrt{\left(\frac{K_I}{K_{II}} \right)^2 + 8} \right) & \text{for } K_{II} > 0 \end{cases} \quad (7^*)$$

Enfoque multiparamétrico.

$$[K_I \sin \theta + K_{II}(3 \cos \theta - 1)] - \frac{16 T}{3} \sqrt{2\pi r} \cos \theta \sin \frac{\theta}{2} = 0 \quad (8^*)$$

Para despejar el ángulo de iniciación de la expresión anterior se han utilizado programas matemáticos de ordenador. (9*)

1.6.2 Criterio de mínima densidad de energía. (SED)

Este criterio se basa en la densidad de energía local en las proximidades de la grieta. La grieta se propagará en la dirección de menor energía. Matemáticamente, esta condición se expresa:

$$\frac{\delta S}{\delta \theta} = 0 ; \quad \frac{\partial^2 S}{\partial \theta^2} < 0 \quad (10^*)$$

Donde S es la energía de deformación

$$S = \frac{1}{2\mu} \left[\frac{\kappa+1}{8} (\sigma_{rr} + \sigma_{\theta\theta})^2 - \sigma_{rr}\sigma_{\theta\theta} + \sigma_{r\theta}^2 \right] \quad (11^*)$$

Como en el criterio anterior se hace una comparación entre los diferentes enfoques, obteniendo el ángulo de iniciación de propagación de la grieta.

Enfoque uniparamétrico.

$$\theta = \arctg \left(\frac{2 K_I K_{II}}{K_I^2 + K_{II}^2} \right) \quad (12^*)$$

Enfoque multiparamétrico.

$$\begin{aligned} \frac{\delta S}{\delta \theta} = & \frac{K_I^2}{16 \mu \pi r} [(\kappa - \cos \theta)(1 + \cos \theta)] + \frac{K_I K_{II}}{8 \mu \pi r} \sin \theta [(1 - \kappa) + 2 \cos \theta] \\ & + \frac{K_{II}^2}{16 \mu \pi r} [(1 + \kappa)(1 - \cos \theta) + (1 + \cos \theta)(3 \cos \theta - 1)] \\ & + \frac{K_I T}{4 \mu \sqrt{2\pi r}} \cos \frac{\theta}{2} [(\kappa - 2) - \cos \theta + 2(\cos \theta)^2] \\ & - \frac{K_{II} T}{4 \mu \sqrt{2\pi r}} \sin \frac{\theta}{2} [\kappa + \cos \theta + 2(\sin \theta)^2] + \frac{1 + \kappa}{16 \mu} T^2 \end{aligned} \quad (13^*)$$

Debido a la complejidad de la expresión, para el enfoque multiparamétrico, el ángulo se obtendrá con programas matemáticos de ordenador.

1.6.3 Criterio de desplazamiento en la punta de grieta. (CTO)

En este criterio, la fuerza conductora es el vector desplazamiento de la punta de grieta. Este vector es la suma del vector de apertura (modo I) y el de deslizamiento (modo II):

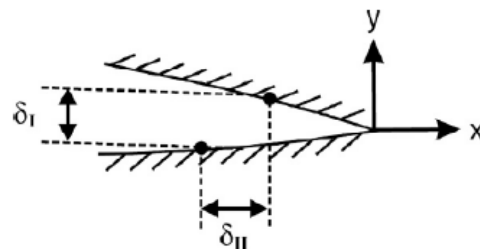


Figure 8. Displacements of two coincident nodes in a loaded crack. [3]

Matemáticamente, se puede calcular el ángulo de iniciación de grieta a través de las siguientes expresiones matemáticas:

$$\operatorname{tg} \theta = \frac{\delta_{II}}{\delta_I} \quad (14^*)$$

$$\operatorname{tg} \theta = \frac{K_{II}}{K_I} \quad (15^*)$$

Donde δ representa las variaciones de desplazamiento de dos nodos coincidentes en las caras de la grieta.

1.7 Metodología en software ANSYS.

Se ha utilizado el software ANSYS para simular las geometrías y estados de carga. Este programa permite calcular los factores intensidad de tensión y el factor *tensión-T*. Sus métodos de cálculo se pueden encontrar en el asistente de ayuda que proporciona el programa.

1.8 Modelo numérico.

Muchos estudios recientes se están centrado en el modo mixto de carga, pero no existen probetas normalizadas para los ensayos.

Se ha utilizado el software ANSYS para modelar la geometría de la probeta, así como las condiciones de contorno necesarias para simular el estado biaxial de tensiones.

- Geometría

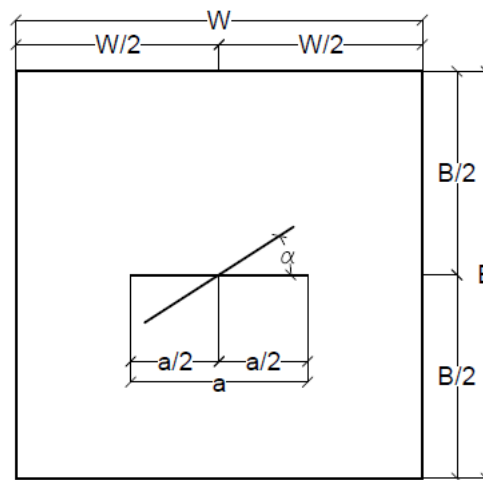


Figure 10. Specimen dimension. ($B = W = 180 \text{ mm}$)

Se trata de un espécimen con sección cuadrada con altura (B) y anchura (W) igual a 180 mm . La grieta se encuentra en el centro de la probeta y su ratio varía entre $a/W = \{0.1-0.9\}$ cada 0.1 . Se ha variado el ángulo de la grieta $\alpha = \{0^\circ-45^\circ\}$ cada 9° .

- Tipo de elemento en ANSYS y material.

El tipo de elemento utilizado para simularlo en ANSYS ha sido PLANE182. Este tipo de elemento se utiliza en elementos con mallas irregulares. Cada nodo tiene dos grados de libertad, movimiento horizontal y vertical.

EL material utilizado es un tipo de hormigón con las siguientes propiedades mecánicas: Módulo de Young $E=40 \text{ GPa}$, y coeficiente de Poisson $v=0.3$. El hormigón es un material quasi-frágil por lo que no sigue el comportamiento elástico lineal.

- Metodología en ANSYS.

Para modelar la probeta en ANSYS se ha tenido especial interés en el modelo alrededor de la grieta. Para simular la grieta y la punta de grieta se han utilizado comandos especiales de ANSYS que más adelante han permitido el cálculo de los parámetros necesarios para el cálculo del ángulo de iniciación de grieta. Como se puede ver en la figura (15*) se ha modelado la grieta mediante dos líneas coincidentes (L13 y L14). Para simular la punta de grieta, que es la región donde se calcula el factor intensidad de tensiones se han utilizado puntos radiales alrededor de la punta de grieta (KP1). Los pasos que se han seguido son los siguientes:

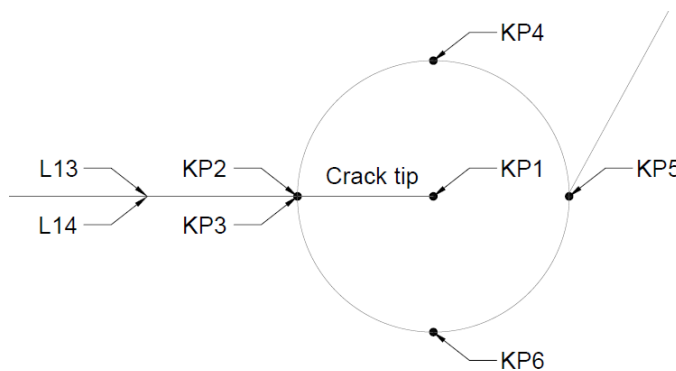


Figure 15. Distribution of keypoints and lines on right crack tip.

1.-Creación de puntos y líneas.

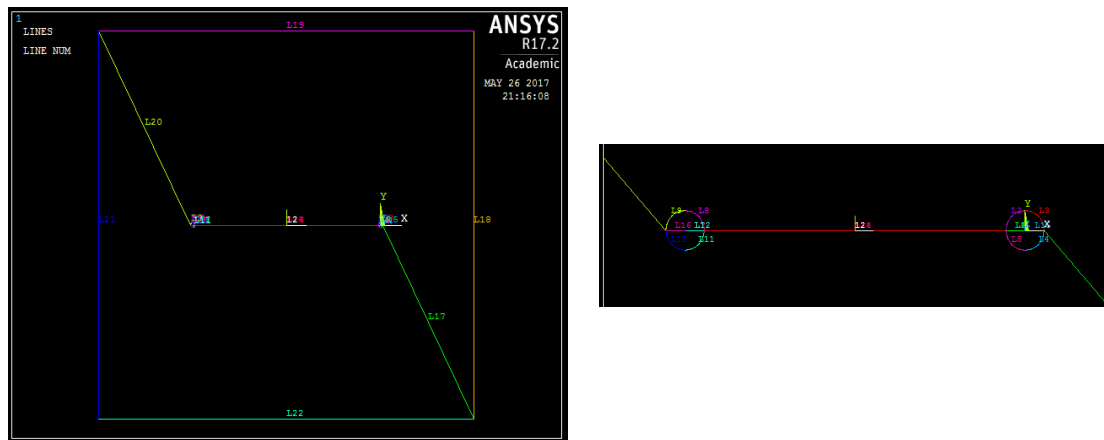


Figure 16. Modeling of specimen. Lines.

2.- Creación de seis áreas que delimitan la grieta.

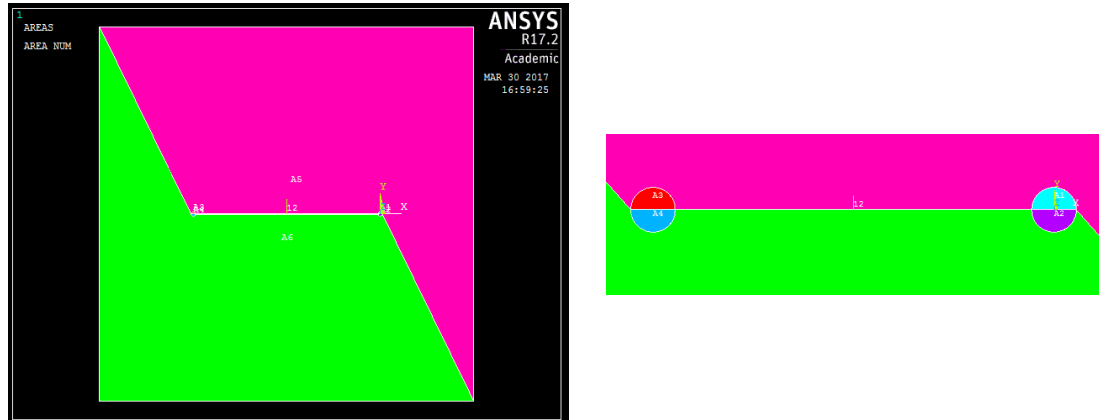


Figure 17. Detail of areas near crack tip.

3.-Mallado del área del modelo.

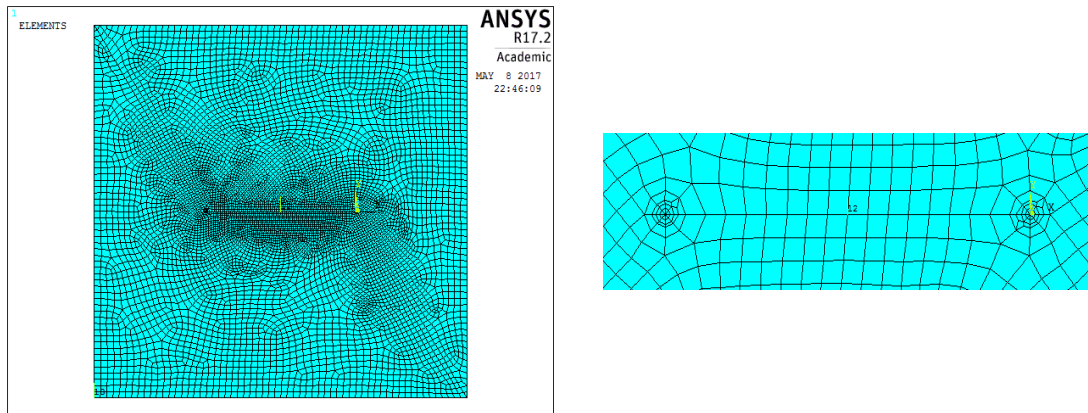


Figure 20 Creating model. *Meshing.* de las áreas.

- Condiciones de contorno

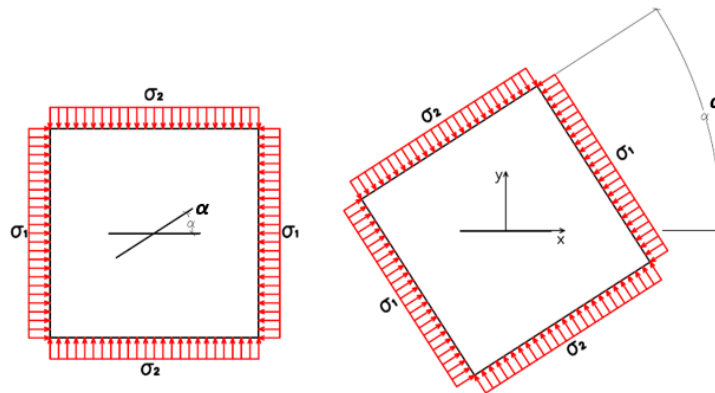
El estado biaxial se ha simulado aplicando presión perpendicular a las superficies del elemento. Dada la metodología de ANSYS ha sido más fácil rotar toda la pieza mediante el uso de ejes polares, que rotar la grieta por lo que ha sido el método utilizado (Figura...).

La presión aplicada en las caras superior e inferior ha sido $\sigma_2=100\text{ MPa}$, mientras que en las caras laterales se ha variado la presión siguiendo las siguientes expresiones:

$$\sigma_2 = 100 \text{ MPa}$$

$$\sigma_1 = \frac{\sigma_1}{\sigma_2} \sigma_2$$

$$\frac{\sigma_1}{\sigma_2} = \{-1; -0.5; 0; 0.5; 1\}$$



Por otro lado, siguiendo el Principio de Acción y Reacción, las condiciones de contorno se han aplicado en ANSYS como se puede ver en la siguiente **Figure 21***

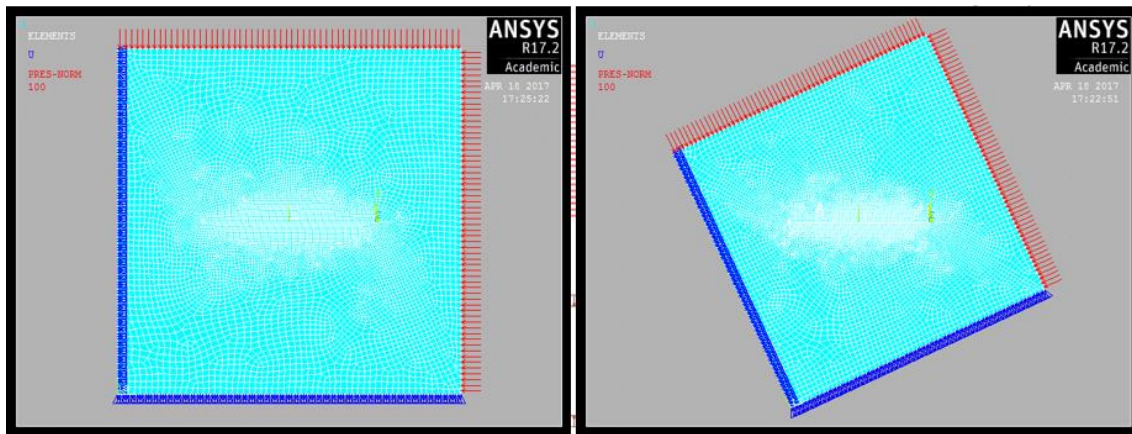


Figure 21 Boundary conditions for different angles (supports and loads)

Las flechas rojas son la presión, siempre perpendicular a las caras, mientras que los triángulos azules son soportes simples.



1.9 Resultados.

Se han utilizado muchas geometrías y situaciones de carga diferentes para predecir el ángulo de iniciación de la grieta. Por otra parte se han utilizado diferentes criterios y programas computacionales para llegar a los resultados como ANSYS y Wolfram Mathematica.

La siguiente tabla resume los criterios utilizados:

	K_I	K_{II}	T-stress	δ_I	δ_{II}	S_1	Enfoque
MTS	X	X					MTS enfoque uniparamétrico.
	X	X	X				MTS enfoque multiparamétrico.
						X	Método de elementos finitos. Método directo MTS.
SED	X	X					SED enfoque uniparamétrico.
	X	X	X				SED enfoque multiparamétrico.
CTOD	X	X					Método de elementos finitos (enfoque uniparamétrico).
				X	X		Método de elementos finitos (enfoque uniparamétrico).

Table 1. Comparison of different criteria

Geometrías y condiciones de contorno utilizadas:

- Casos de carga:**

$$\sigma_1/\sigma_2 = \{-1; -0.5; 0; 0.5; 1\}$$

- Ratio de longitud de grieta:**

$$a/W = \{ 0.1; 0.2; 0.3; 0.4; 0.5; 0.6; 0.7; 0.8; 0.9 \}$$

- Inclinación de grieta:**

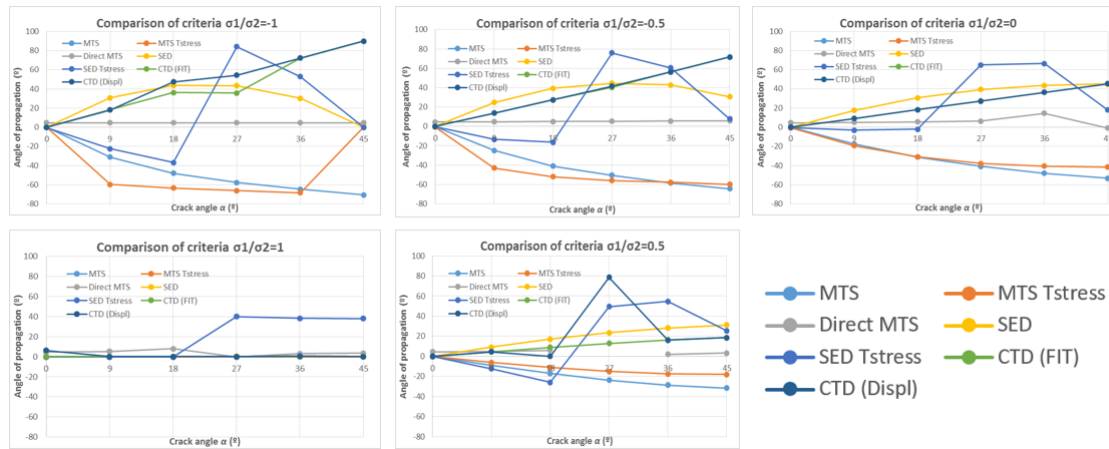
$$\alpha = \{ 0^\circ; 9^\circ; 18^\circ; 27^\circ; 36^\circ; 45^\circ \}$$

Método de obtención de cada parámetro:

- Factor intensidad de tensiones: El valor de este factor nos indica a qué modo de carga está sometido el elemento. Cuando el valor de K_I es muy grande nos indica que está sometido a modo I o de apertura y lo mismo con el modo II y el factor K_{II} . Los valores obtenidos se pueden ver en las tablas Table 2 a Table 4 del proyecto. (Páginas 45 a 47)
- Tensión-T: Este parámetro se ha obtenido con ANSYS. La evolución de la tensión-T con respecto a los diferentes casos de carga y longitud de grieta se pueden observar en los gráficos Graph 1. a Graph 10. (Páginas 51 y 52).
- Desplazamientos (δ_I y δ_{II}): Se han obtenido en ANSYS. La forma de obtenerlos y algunos resultados se pueden ver en el apartado Displacements (δ_I and δ_{II})
- Tensión principal (S_1): Este factor se ha utilizado para calcular el ángulo de iniciación con el criterio de tensión tangencial máximo de manera directa. La forma de obtenerlos mediante el programa ANSYS y una aproximación mediante regresión polinómica se puede ver más detalladamente en el apartado 5.1.4.-Principal Tensile Stress S_1 .

1.10 Resultados

En este apartado se explican algunos de los resultados obtenidos. Para una información más completa ver el apartado **5.-Results**, donde se presentan tanto en gráficos como en tablas los valores de todos los parámetros anteriormente explicados así como los valores del ángulo de iniciación.

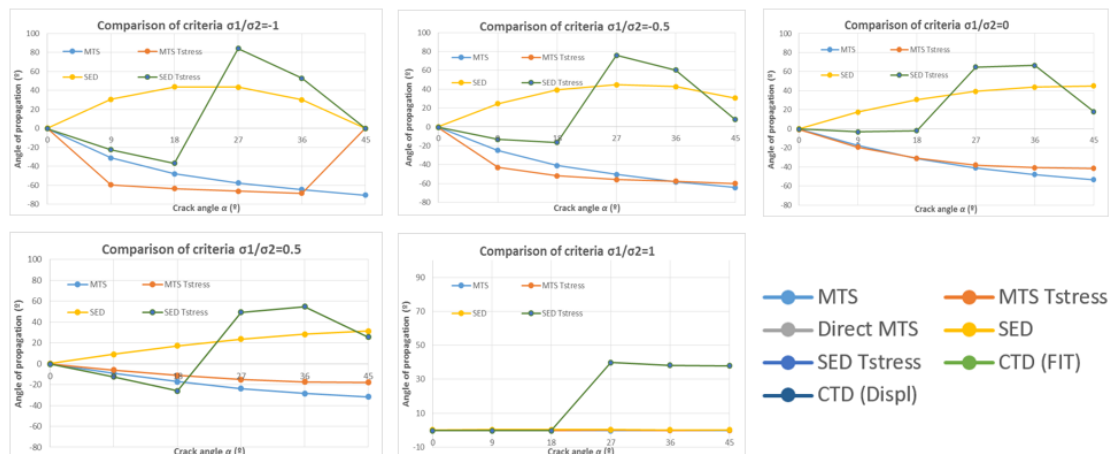


Extractos de Gráficos Graph 26.* a Graph 50.*

Como ejemplo se presentan los siguientes gráficos obtenidos para una geometría de $a/W=0.1$, variando la inclinación de la grieta entre 0° y 45° y con todos los casos de carga presentados anteriormente.

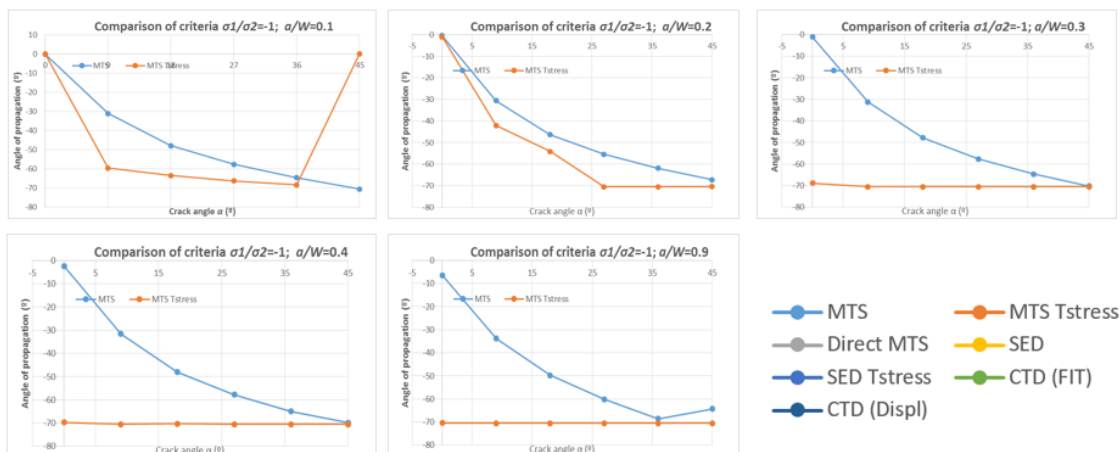
Cada color representa un criterio diferente como se puede leer en la leyenda. Se puede observar una gran desviación de los valores obtenidos que en gran parte se debe a las diferentes hipótesis y los diferentes parámetros que tiene en cuenta cada criterio.

Para observar mejor estas diferencias, se presentan algunos gráficos comparativos.



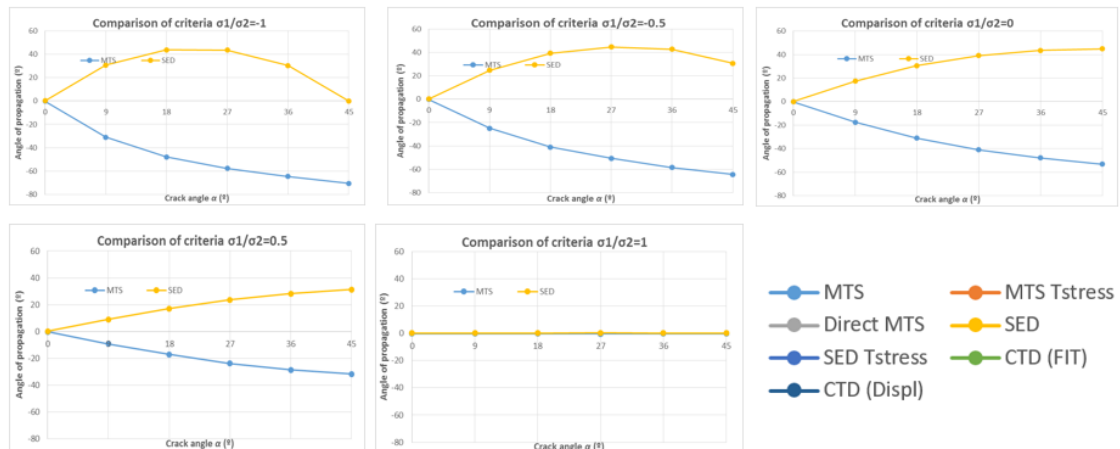
Extractos de Gráficos Graph 26.* a Graph 50.

La adición de la tensión-T en la expansión de Williams es una de las mayores causas de estas diferencias



Extractos de Gráficos Graph 26.*. a Graph 50

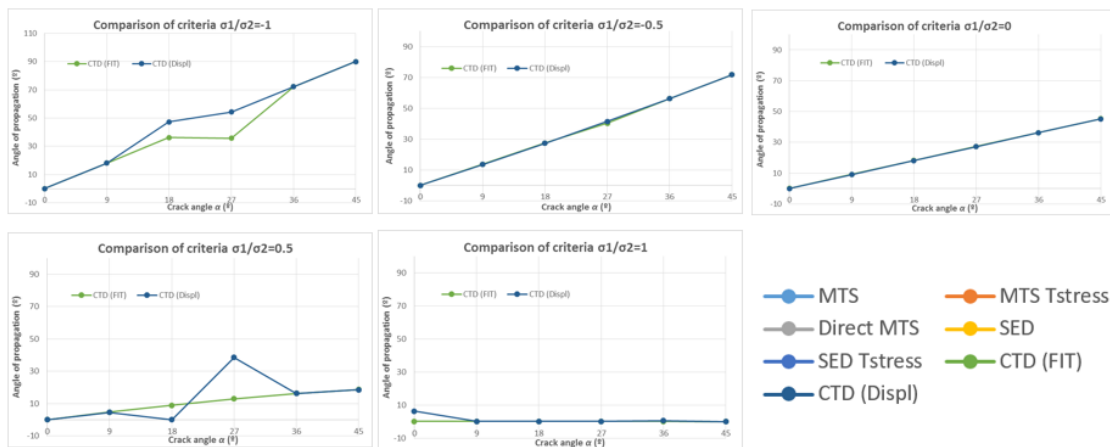
Si se compara el MTS sin el parámetro tensión- T y con él, se puede observar que los valores son similares para ratios de grieta pequeños (0.1-0.2). A partir de ahí los valores se disparan y tienden a un valor constante de 70°.



Extractos de Gráficos Graph 26.*. a Graph 50

Al comparar los criterios MTS y SED en enfoque uniparamétrico, se puede decir que sus valores son comparables para grados menores que 18° o 27° generalmente.

Se puede apreciar que los resultados tienen valores iguales y signos opuestos. Esto se debe a la metodología que utiliza ANSYS para calcular los factores intensidad de tensiones ya que los calcula en valor absoluto. Al ser las ecuaciones de cálculo del ángulo, ecuaciones trigonométrica, estas dependen del signo de los factores intensidad de tensiones.



Extractos de Gráficos Graph 26.*. a Graph 50

Por último se puede apreciar que los ángulos calculados con el criterio del vector de desplazamientos son muy similares.

1.11 Conclusiones

Se ha comprobado que los resultados obtenidos difieren mucho entre sí cuando se comparan diferentes criterios e incluso con el mismo criterio. Esto se debe a diferentes causas:

- Uso de diferentes criterios.
- Metodología de cálculo de cada parámetro:
 - Las ecuaciones complejas se han resuelto con el programa Wolfram Mathematica, que al resolver ecuaciones trigonométricas proporciona varios resultados de los que se ha tenido que elegir el más adecuado.
 - El programa ANSYS trabaja con elementos finitos. El cálculo de elementos finitos siempre conlleva aproximaciones. Por otra parte, para geometrías complejas, como por ejemplo, cuando se rota la geometría, la malla puede ser irregular y generar problemas.
- La solución del ángulo depende de varios parámetros. El cálculo de estos parámetros también ha podido ser problemático:
 - K_I y K_{II} se han obtenido con ANSYS con los errores que puede conllevar
 - LA tensión- T y la tensión principal se han calculado combinando ANSYS y ajustes lineales y polinómicos respectivamente, las cuales siempre conlleva errores.

No existe una conclusión definitiva para determinar que método es el más adecuado para predecir la dirección de propagación de grietas en materiales no lineales pero se puede decir que la adición de parámetros en la expansión de Williams provoca un cambio significativo. Sería necesario un análisis más detallado y profundo. Los ensayos experimentales serían un buen método de ayuda para llegar a conclusiones más claras.

2 Introduction

One of the most important phases in designing engineering components is to set the most likely failure mode. These failures can occur suddenly in the components even when they are oversized in relation to the material resistance theory due to fracture and fatigue processes.

The fracture of a solid can be defined as its separation into two or more parts under the effects of a stress due to the propagation of cracks. Fracture is the consequence of the rupture of existing interatomic bonds in a solid material. These defects condition the properties of the components in service, including their tenacity, brittleness, breaking strength, fatigue resistance or resistance under corrosion.

The classical mechanics of the fracture is based on materials with brittle behavior, which greatly limits the field of application. Recent studies are attempting to find a solution for almost brittle and linear elastic behavior materials. Throughout this project will emphasize the different approaches of fracture mechanics as well as the existing criteria to calculate the angle of propagation of cracks in non-elastic materials. The calculation of the angle of crack propagation can be complex but it is a very important parameter in the design of engineering components. Whether it is known the way in which these components fail, it can be prevented in the design phase of them.

The structure of this document tries to explain step-by-step the different approaches of fracture mechanics, emphasizing the mechanics of non-linear fracture. First of all, there is a comparison of the two types of approaches to deepen in the mechanics of linear elastic fracture. An in-depth analysis of the different existing criteria have been made to predict the direction of crack propagation that have been used to obtain experimental results.

Different mathematical programs (such as Wolfram) and finite element analysis (ANSYS) have been used to obtain results. Since there is no normalized geometry for these experimental results, a geometry has been chosen that will vary in different ratios. Finally the results and the conclusions obtained are presented.

3 Theoretical background

The aim of mechanical fracture is the study and analysis of the mechanical behavior in cracked structural elements. Due to the infinity of different materials and the existence of multiple defects in the specimens, is difficult to predict the failure. It is important to predict how the crack grows and the rate of propagation in order to avoid accidents.

The fracture strength of a solid material is due to the cohesive force that exists between its atoms. From the beginning of the study of the mechanics of the fracture, it was verified that the theoretical and experimental results of fracture resistance diverged considerably. Griffith was the first to propose that the discrepancy between theoretical and experimental resistance was explained by the presence of microscopic cracks, which always exist under normal conditions on the surface and interior of a piece. All of these defects work as stress concentrators at their ends, producing stresses much greater than those applied, reason why, the fracture can happen long before what theoretically expected. The fracture will be produced when the stress overcome the material resistance. [6]

All mechanical elements present defects in their composition; bigger or smaller cracks which their propagation could be dangerous in their service, because lot of them are almost impossible to detect. It is necessary to know the behavior of cracked components under service loads and determinate the security grade in each case [6]. The study of cracked components is usually based on probability inasmuch as without destructive tests, we only can be sure that there are not bigger defects than the sensitivity of our method of inspection.

3.1 Loading modes

The fracture mechanics is based on the calculation of the field of stress and deformations around the vicinity of a crack, which causes the relative displacement of the fracture surfaces in a body.

Any relative movement of the surfaces of a fissure can be obtained as a combination of three basic movements. There are three modes of loading which can individually or simultaneously affect cracked components:

- Mode I or opening mode (Figure 1 A): Principal load is applied normal to the crack plane.
- Mode II or sliding mode (Figure 1 B): The stress is parallel to the plane of the crack and it is applied on the shear plane. Corresponds to in-plane shear loading and tends to slide one crack face with respect to the other

- Mode III or tearing mode (Figure 1 C): The stress is parallel to the plane of the crack and it is applied out of the shear plane.

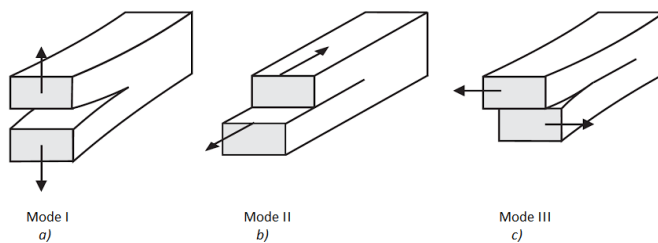


Figure 1 Charging modes (a) mode I (or opening mode), (b) mode II (or sliding mode), (c) mode III (or tearing mode)

The general case is the combination of the three charging modes, which is very complicated to analyze. A great number of the fatigue crack growth studies are commonly performed under mode-I loading conditions. However, single-mode loading rarely occurs in practice, and in many cases cracks are not normal to the maximum stress [4].

Mode-I or opening mode only occurs when the tension applied is perpendicular to the faces of the crack. However, a combination of great interest is that of mode I and II which can occur when the crack is inclined with respect to the applied loads [15]. Moreover, defects on the specimen are often randomly oriented and located which develop in a mixed mode state [5]. One example is an initial crack not orthogonal to the applied normal stress (Figure 2). As the crack orientation is not perpendicular to the uniaxial stress, the state of loading is a combination of mode I and II. However, as it is shown in the Figure 2, the crack tends to propagate normal to the applied load, resulting in pure Mode I loading [7].

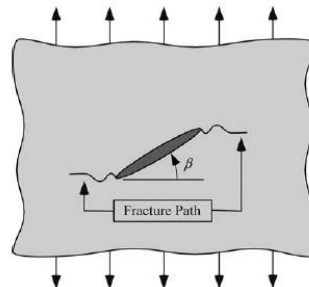


Figure 2. Bidimensional model under uniaxial load conditions

From the other side, it was found that a crack under mixed-mode loading conditions (Figure 3) will deviates from its original direction [4]. The main characteristic of crack propagation under mixed mode is that, the crack propagates in non-similar manner. Therefore the study of mixed mode is more difficult and the crack initiation angle (see Figure 4) should be taken into account in the design phase of engineering components.

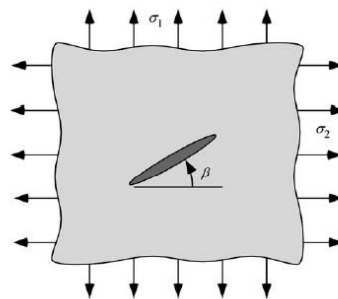


Figure 3. Bidimensional model under biaxial load conditions. Mixed mode (I and II)

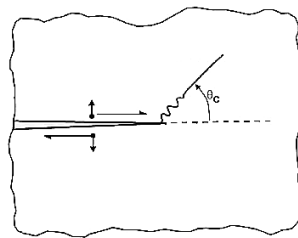


Figure 4. Crack initiation angle (θ) under mixed mode conditions

One characteristic example of mixed mode (I-II) nowadays, is the stress state of railway wheels leads to fatigue in high speed velocity railway. It is a common investigation because fix or replace this kind of steel components is really expensive. Wheel shelling and rail squats (see Figure 5) are examples of defects originated on the railway as a result of wheel rail-rolling contact. A crack in the radial direction propagates under combined mode I (due to the centrifugal forces) and mode II (due to the rolling contact forces and friction) [5].



Figure 5. Squat defects in railway [23]

3.2 Stress intensity factor

To perform the analysis of the fracture, the first step, is the calculation of the field of stresses around the crack, since these are the ones that produce the deformation of the material and create the new surfaces.

The stress intensity factor K is the most significant parameter of the elastic-linear fracture mechanics, since it predicts stress intensity near the tip of a crack caused by a remote load or residual stresses. K therefore, determines the effect of introducing a crack into a structure. Since once it has known K , the field of stress around the crack is completely defined [15].

The magnitude of K depends on several parameters as:

- Sample geometry.
- Size and location of the crack.
- Magnitude of load.
- Distribution of load.

If an arbitrary component with a crack of any size and geometry committed to stress is considered, we are able to calculate the tensional field near to the crack front. Polar coordinates are used to define the location of any point respect to the crack tip using r (radius) and θ (angle) (See Figure 6). From there, many authors such as Westergaard, Irwin, Sneddon, and Williams have postulated a series of terms to define the field of stresses near to the crack assuming isotropic linear elastic material behavior [7]:

$$\sigma_{ij} = \left(\frac{k}{\sqrt{r}}\right) f_{ij}(\theta) + \sum_{m=0}^{\infty} A_m r^{\frac{m}{2}} g_{ij}^{(m)} \quad i, j \in \{x, y\}, \quad (16)$$

where

σ_{ij} = stress tensor

r and θ are the polar coordinates defined in Figure 6

k = constant

$f_{ij}(\theta)$ = dimensionless function of θ in the leading term

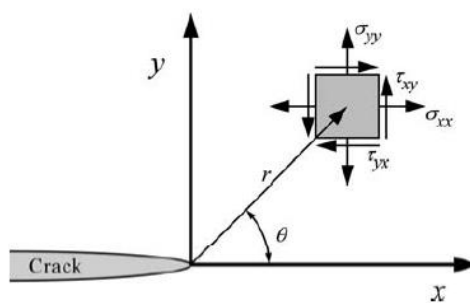


Figure 6. Definition of the coordinate axis ahead of a crack tip. x direction is normal to the page [7]

When a structural component is stressed in tension or bending, the developed stress field in the vicinity of crack tip under elastic conditions shows a singularity following an inverse square root relationship with the distance from the crack tip (as it is shown on the equation (16)) [12].

Each mode of loading presented previously, produce the singularity at the crack tip, but k and f_{ij} depend on the mode. k can be replaced by the **stress intensity factor K** , where $K = k\sqrt{2\pi}$ (KI, KII, KIII for each mode). In the case of mixed mode (I+II) the individual contribution to a given stress component are additive (principle of linear superposition, equation (17)) [7]:

$$\sigma_{ij}^{(total)} = \sigma_{ij}^{(I)} + \sigma_{ij}^{(II)} \quad (17)$$

3.3 T-Stress

Another parameter that allows us to characterize the level of constraint and the fields of stresses and displacements around the crack tip is T-stress. This parameter, in plane conditions, represents the stress parallel to the crack line. Generally, the stress intensity factor is enough to characterize the field of stress and displacements in a geometry, but there are some cases where the parameter T-stress can be large in comparison with the other parameters, reason why it is important to take it into account. [20]

One of these cases is the one that occupies this thesis, when the crack is inclined with respect to the action of the loads. The T-stress factor can have a significant effect on the size and shape of the plastic zone that develops around the crack bridge. Therefore, T-stress is used as the second parameter to fully characterize the crack tip. [20]

There are many methods to calculate T-stress. One of them, it can explain referring to the characterization of the crack tip by polar coordinates and the following equation (18):

$$T = (\sigma_{xx} - \sigma_{yy})_{\theta=0}, \quad (18)$$

where σ_{xx} and σ_{yy} represent the stress components along the axis x and y respectively, and θ is the polar coordinate angle.

This equation means that for θ equals to zero (see Figure 7), T-stress can be calculated by the difference between σ_{xx} and σ_{yy} components.

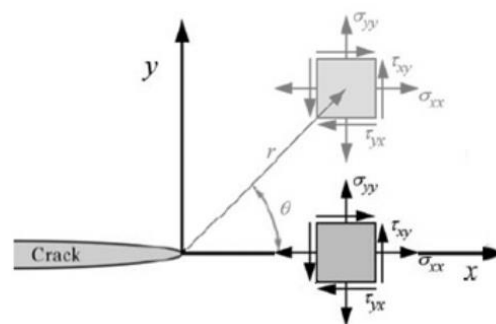


Figure 7. Definition of polar coordinates with angle theta equal to zero. ($\theta = 0$) [7]

3.4 Single-parameter and multi-parameter approach

The traditional classic linear elastic fracture (also called, single-parameter) describe the stress distribution field in cracked components in terms of stress intensity factor. Is one of the most common used theory for assessment of fracture behavior of several structures and materials [17].

Is it called single-parameter because the stress intensity factor is the only parameter which is taken into account and is sufficient to define the stress and displacement field near to the crack tip. Moreover, is derived for brittle materials and its rather investigated [18].

However, LEFM has several limitations. Among them, the most important is that the extent of the zone of non-linear behavior that has to be small enough in comparison to the typical structural dimensions [9]. For big amount of materials such as quasi-brittle or elastic-plastic materials this restriction is too strong because there are many parameters which have to be taken into account in the process of their fracture such as, heterogeneities, pores, microcracks or other defects [3]. If the nonlinear behavior is of a large extent the size/geometry/boundary effect cannot be omitted [17].

The objective of this project is in conflict with this limitation since the material of the study of the specimen is concrete. More information on the material can be found in the subsection [4.6. Material properties]. Concrete can be classified as a quasi-brittle material. In general, the fracture process of this type of material is characterized by the existence of a large fracture zone. Thus, the principles of the conventional linear elastic fracture mechanics concept, are not valid for this case. [18]

The so-called **multi-parametric approach** is used in order to avoid these problems. Using more than one or two parameters to approximate the stress and displacement fields present a great advantage for materials with quasi-brittle and elastic-plastic behavior.

3.5 Williams expansion

The multi-parametric approach is based on Williams expansion. The Williams solution of the crack-tip stress and displacement field distribution in a cracked specimen provides a reasonable approximation [3]. It is expressed in a form of a series expansion, particularly as a power series. This solution was originally delivered for a homogeneous elastic isotropic cracked material with an arbitrary remote loading.

$$\sigma_{ij} = \sum_{n=1}^{\infty} \frac{n}{2} r^{\frac{n}{2}-1} A_n f_{ij}^{\sigma}(\theta, n) + \sum_{m=1}^{\infty} \frac{m}{2} r^{\frac{m}{2}-1} B_m g_{ij}^{\sigma}(\theta, m) \quad i, j \in \{x, y\} \quad (19)$$

$$u_i = \sum_{n=0}^{\infty} r^{\frac{n}{2}} A_n f_i^u(\theta, n, E, v) + \sum_{m=0}^{\infty} r^{\frac{m}{2}} B_m g_i^u(\theta, m, E, v) \quad i, j \in \{x, y\} \quad (20)$$



The first (singular) term coefficients A_n and B_m in equations (19) and (20) are related to mode I and mode II stress intensity factor (K_I and K_{II} respectively), where $KI = An \sqrt{2\pi}$ and $KII = -Bm \sqrt{2\pi}$. These parameters are dominant for $r \rightarrow 0$, which is the main idea of the conventional LEFM approach [18]. They depend on the specimen geometry, relative crack length α and loading conditions [17].

The center of the polar coordinates system $(r; \theta)$ is at the crack tip (see Figure 6). E and v represent material properties (Young's modulus and Poisson's ratio). f_{ij}^{σ} , g_{ij}^{σ} , f_i^u and g_i^u are known functions corresponding to the stress and displacement distribution and to the loading mode I (f) and mode II (g), respectively.

The higher-order terms in Williams expansion can have a significant effect on the crack growth path prediction so that it is useful to add more parameters into the numerical calculation.

When more than only the first term of the Williams expansion shall be taken into account for application of those criteria, such an approach is referred to as the multi-parameter form.

Coefficients of the higher order terms $n, m > 1$ can contribute to a more reliable utilization of the fracture resistance value obtained from measurements on laboratory specimens within the fracture behavior assessment of a real structure [18]. These parameters are really significant especially when the nonlinear zone extent around the crack tip is large.

The main purpose of this paper is to study the influence of the addition of more than one parameter on Williams expansion in a specimen under mixed mode loads to observe the crack angle propagation. To do this, by developing the Williams expansion for the stress field (18) and substituting the values of the stress factors, the following equations (21) and (22) are obtained:

$$\sigma_{ij} = \frac{K_I}{\sqrt{2\pi r}} f_{ij}^I(\theta) + \frac{K_{II}}{\sqrt{2\pi r}} f_{ij}^{II}(\theta) \quad (21)$$

$$\sigma_{ij} = \frac{K_I}{\sqrt{2\pi r}} f_{ij}^I(\theta) + \frac{K_{II}}{\sqrt{2\pi r}} f_{ij}^{II}(\theta) + T \delta_{1i} \delta_{1j} \quad (22)$$

The equation (21) refers to the aforementioned LFME since it only takes into account the first two singular terms of the Williams expansion. K_I and K_{II} are the only parameters that are taken into account to describe the behavior caused by normal and tangential stresses.

On the other hand, equation (22) refers to the multi-parametric approach since it includes also, the T-stress parameter (T) that is defined as the first term of the non-singular terms in the normal stress component parallel to the crack plane at the crack tip.

In both equations (21) and (22) $f_{ij}(\theta)$ are known angular functions.

In the next section, three criteria for estimating the direction of crack growth under mixed mode are to be introduced. A comparison between the application of the criteria under the multi and single-parametric approach will be made.

3.6 CRITERIA FOR PREDICTION OF ANGLE PROPAGATION.

Over the time, many criterions have been proposed to explain cracks propagation. Some of the specimens fit only under mode I, while other can be expanded to mixed load.

The maximum tangential stress (MTS), the minimum strain energy density (SED), and the vector crack tip displacement (CTD) are widely used and investigated by many authors. In them, it is analyzed which is the driving force of growth direction. The criteria are based on the fact that crack propagation will start when the loads reach a value such, that the characteristic parameter of the model is critical. The propagation will continue as long as it exceeds that value.

As two different approach have been explained, the analysis of the criteria will be focus on both point of view.

3.6.1 Maximum tangential stress criterion (MTS criterion)

It is one of the most commonly used criteria. It was proposed by Erdogan and Sih [11]. It assumes that a crack will propagate in the direction with maximal tangential stress [3]. It is stress-based criteria, so it does not depend on plane stress/strain conditions. This criterion states that crack propagation starts from the crack tip along the radial direction $\theta=\theta_c$ on which tangential stress σ_θ become maximum (see Figure 6) [5]

Mathematically, this condition can be expressed as:

$$\frac{\partial \sigma_{\theta\theta}}{\partial \theta} = 0 \quad \text{and} \quad \frac{\partial^2 \sigma_{\theta\theta}}{\partial \theta^2} < 0. \quad (23)$$

Using equations (20) and (21) to describe the field near the crack tip (Williams expansion), and applying the MTS criterion condition as shown in equation (23) the following equations can be obtained. They will allow to calculate the crack initiation angle for single and multi-parametric approaches ((24), (25) and (27), (28) respectively):

Single-parameter approach

$$K_I \sin \theta + K_{II} (3 \cos \theta - 1) = 0 \quad (24)$$

$$\theta = \begin{cases} 2 \arctg \frac{1}{4} \left(\frac{K_I}{K_{II}} + \sqrt{\left(\frac{K_I}{K_{II}} \right)^2 + 8} \right) & \text{for } K_{II} < 0 \\ 0 & \text{for } K_{II} = 0 \\ 2 \arctg \frac{1}{4} \left(\frac{K_I}{K_{II}} - \sqrt{\left(\frac{K_I}{K_{II}} \right)^2 + 8} \right) & \text{for } K_{II} > 0 \end{cases} \quad (25)$$

From multi-parametric point of view, the also-called modified MTS criterion takes into account the T-stress parameter while previously, the conventional MTS criterion takes into account only

the singular term in William's expansion [21]. If the angular functions $f_{ij}(\theta)$ are substituted on equation (22)(22), the tangential stress in the vicinity of a crack tip subjected to mixed mode can be written as (26)

$$\sigma_{\theta\theta} = \frac{1}{\sqrt{2\pi r}} \cos \frac{\theta}{2} \left[K_I \cos^2 \frac{\theta}{2} - \frac{3}{2} K_{II} \sin \theta \right] + T \sin^2 \theta \quad (26)$$

According to the equation (23), and deriving the previous equation:

Multi-parameter approach

$$[K_I \sin \theta + K_{II}(3 \cos \theta - 1)] - \frac{16 T}{3} \sqrt{2\pi r} \cos \theta \sin \frac{\theta}{2} = 0 \quad (27)$$

To obtain the angle of the above equation, very complex mathematical methods are required which are not included in this paper. An alternative way to obtain it is by using numerical computer software. In this case Wolfram Mathematica Software has been used.

3.6.2 Minimum strain energy density SED CRITERIA

This criterion was proposed by Sih [13] and is based on the local density of the energy field in the crack tip region [5]. The information about the plane strain/stress condition is really important in this case inasmuch as handles with strain energy density. Mathematically, this condition is expressed like [3]:

$$\frac{\delta S}{\delta \theta} = 0 ; \quad \frac{\partial^2 S}{\partial \theta^2} < 0 \quad (29)$$

where S is the strain energy density and it can be expressed like :

$$S = \frac{1}{2\mu} \left[\frac{\kappa+1}{8} (\sigma_{rr} + \sigma_{\theta\theta})^2 - \sigma_{rr}\sigma_{\theta\theta} + \sigma_{r\theta}^2 \right] \quad (30)$$

Where,

μ is the shear modulus.

$\kappa = \frac{3-\nu}{1+\nu}$ in plane strain conditions.

σ_{rr} and $\sigma_{\theta\theta}$ are the stress components along the radial and tangential direction (refers to polar coordinates in Figure 6)

As in the previous criterion, the comparison between single and multi-parameter criteria will be explain.

The following equations allow to obtain the angle of propagation of the crack for the different approaches. To obtain this equations Williams expansion and the expression of displacements and stresses close to the crack tip from loading modes I and II, have been used. This equations can be found in [19]. A more detailed treatment to predict the crack trajectories by using strain energy density function can be found in [19] and in [22].

As in this project, the values of stress intensity factor (K_I and K_{II}) will be use, the following equation is referred to them.

$$\theta = \arctg \left(\frac{2 K_I K_{II}}{K_I^2 + K_{II}^2} \right) \quad (31)$$

Following the same procedure, the function used to calculate the angle of propagation in multi-parametric approach, taking into account T-stress parameter:

$$\begin{aligned} \frac{\delta S}{\delta \theta} = & \frac{K_I^2}{16 \mu \pi r} [(\kappa - \cos \theta)(1 + \cos \theta)] + \frac{K_I K_{II}}{8 \mu \pi r} \sin \theta [(1 - \kappa) + 2 \cos \theta] \\ & + \frac{K_{II}^2}{16 \mu \pi r} [(1 + \kappa)(1 - \cos \theta) + (1 + \cos \theta)(3 \cos \theta - 1)] \\ & + \frac{K_I T}{4 \mu \sqrt{2 \pi r}} \cos \frac{\theta}{2} [(\kappa - 2) - \cos \theta + 2(\cos \theta)^2] \\ & - \frac{K_{II} T}{4 \mu \sqrt{2 \pi r}} \sin \frac{\theta}{2} [\kappa + \cos \theta + 2(\sin \theta)^2] + \frac{1 + \kappa}{16 \mu} T^2 \end{aligned} \quad (32)$$

Due to the complexity of the expression, the solution has been sought numerically with Wolfram Mathematica Software.

3.6.3 The CTD criterion

The vector crack tip displacement (CTD) was proposed by Li and it is based on the concept that the vector crack tip displacement is the driving force for fatigue crack growth. This vector is the summation of the opening displacement vector (mode I) and the sliding displacement vector (mode II). The crack is assumed to propagate along the direction of this vector [3].

$$\operatorname{tg} \theta = \frac{\delta_{II}}{\delta_I} \quad (33)$$

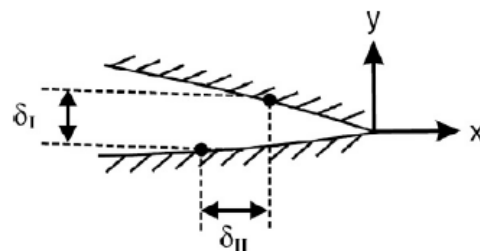


Figure 8. Displacements of two coincident nodes in a loaded crack. [3]

Where δ represent differences of the displacements of two coincident nodes selected at the crack faces (with the same x, y coordinates before the load is applied). This displacements are

shown in Figure 8. Equation (33) can be expressed also by means of the stress intensity factor when classical single-parameter is considered:

$$\operatorname{tg} \theta = \frac{K_{II}}{K_I} \quad (34)$$

Multi-parametric approach of CTOD criterion is not contemplated on this project but it also can be obtained using Williams expression using the field of displacements by means of equation (20)

3.7 ANSYS METHODOLOGY

The commercial software ANSYS has been used to obtain the stress intensity factors and the T-stress. In the following section it will be explained how ANSYS calculates these parameters.

3.7.1 KCALC. Stress Intensity Factors in ANSYS

KCALC command calculates the stress intensity factors in fracture mechanics analyses. The software uses a nodal displacement extrapolation in the calculation. The analysis uses a fit of the nodal displacements in the vicinity of the crack. The actual displacements at and near a crack for linear elastic materials are based on Paris and Sih postulations [8]:

$$u = \frac{K_I}{4G} \sqrt{\frac{r}{2\pi}} \left((2k-1) \cos \frac{\theta}{2} - \cos \frac{3\theta}{2} \right) - \frac{K_{II}}{4G} \sqrt{\frac{r}{2\pi}} \left((2k+3) \sin \frac{\theta}{2} + \sin \frac{3\theta}{2} \right) + O(r) \quad (35)$$

$$v = \frac{K_I}{4G} \sqrt{\frac{r}{2\pi}} \left((2k-1) \sin \frac{\theta}{2} - \sin \frac{3\theta}{2} \right) - \frac{K_{II}}{4G} \sqrt{\frac{r}{2\pi}} \left((2k+3) \cos \frac{\theta}{2} + \cos \frac{3\theta}{2} \right) + O(r) \quad (36)$$

$$w = \frac{K_{III}}{G} \sqrt{\frac{r}{2\pi}} \sin \frac{3\theta}{2} + O(r) \quad (37)$$

Where

u, v, w , are the displacements in a local Cartesian coordinate system.

r, θ , are coordinates in local cylindrical coordinate system.

G , shear modulus.

K_I, K_{II}, K_{III} , stress intensity factors

$O(r)$, terms of order r or higher

As the model used on this study will be full-crack model, the stress intensity factors are calculated as:

$$K_I = \sqrt{2\pi} \frac{G}{1+k} \frac{|\Delta v|}{\sqrt{r}} \quad (38)$$

$$K_{II} = \sqrt{2\pi} \frac{G}{1+k} \frac{|\Delta u|}{\sqrt{r}} \quad (39)$$

$$K_{III} = \sqrt{2\pi} \frac{G}{1+k} \frac{|\Delta w|}{\sqrt{r}} \quad (40)$$

Where $\Delta v, \Delta u, \Delta w$ are the motion of one crack face with respect to the other.

The nodes used for the approximate crack-tip displacements have to be selected like is shown on the Figure 9 through PATH command on ANSYS Software.

3.7.2 PATH command

The **PATH** command is used to define parameters for establishing a path. In order to calculate the stress intensity factor, the way to create the path is the following:

The first node on the path should be the crack-tip node (I on Figure 9). For a full-crack model, where both crack faces are included, four additional nodes are required: two along one crack face (J,K) and two along the other (L,M). [8]

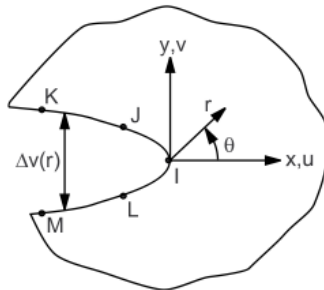


Figure 9. Path for KCALC [8]

This command has been used also for obtain results of different parameters and stresses near to the crack tip. (More information in subsection 9.2.How to get each parameter)

4 Numerical model

Although more and more studies are focused on mixed mode, there is no standardizes tests. Many geometries and different applied forces are used to simulate the mixed mode in order to analyze the propagation of the crack [5].

The commercial software ANSYS has been used to model the geometry with the aim of finding K_I and K_{II} values and to calculate the direction of propagation under mixed mode, using different combination of loads (σ_1 and σ_2)

ANSYS software and especially ANSYS Mechanical APDL is a finite element tool for structural analysis. It is used to predict how the element will work and react under a real environment.

Since the purpose is to know the angle of propagation of the crack, it is analyzed and explained in what criteria and basis the software ANSYS is based to obtain the stress intensity factors (K_I and K_{II}). First of all, it is necessary to detail the process of creating the model.

4.1 Specimen geometry and dimensions

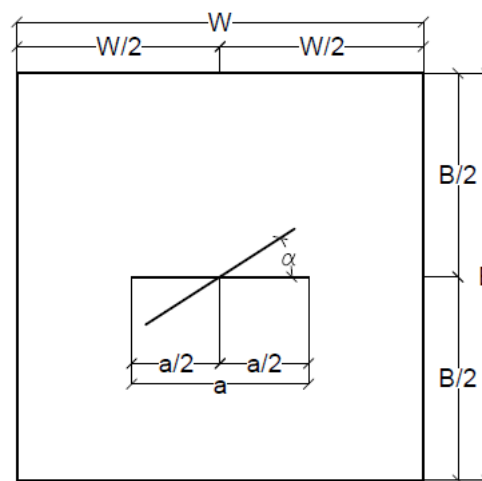


Figure 10. Specimen dimension. ($B = W = 180$ mm)

A square bidimensional model with plane strain conditions has been used for the investigation (see Figure 10). The main dimensions of the geometry are B and W , which are the same and equal to 180 mm. The specimen presents a centered crack of length a , which varies in a ratio of a/W between 0.1 and 0.9. Moreover, the angle of the crack (α) has been changed from 0° to 45° every 9° .

As the objective of the investigation is to observe the crack propagation angle under mixed mode for different crack angles (α), crack rotation has been simulated with the ANSYS software. To simplify the modeling, it has been chosen to turn the piece instead of the crack (see Figure 11). Thanks to the polar coordinates, it is a simple methodology in which it is only necessary to change one parameter on ANSYS code to simulate it. In this way, the loads (σ_1 and σ_2) remain perpendicular to the faces of the specimen and it is possible to simulate the mixed mode of loading for any crack angle (α).

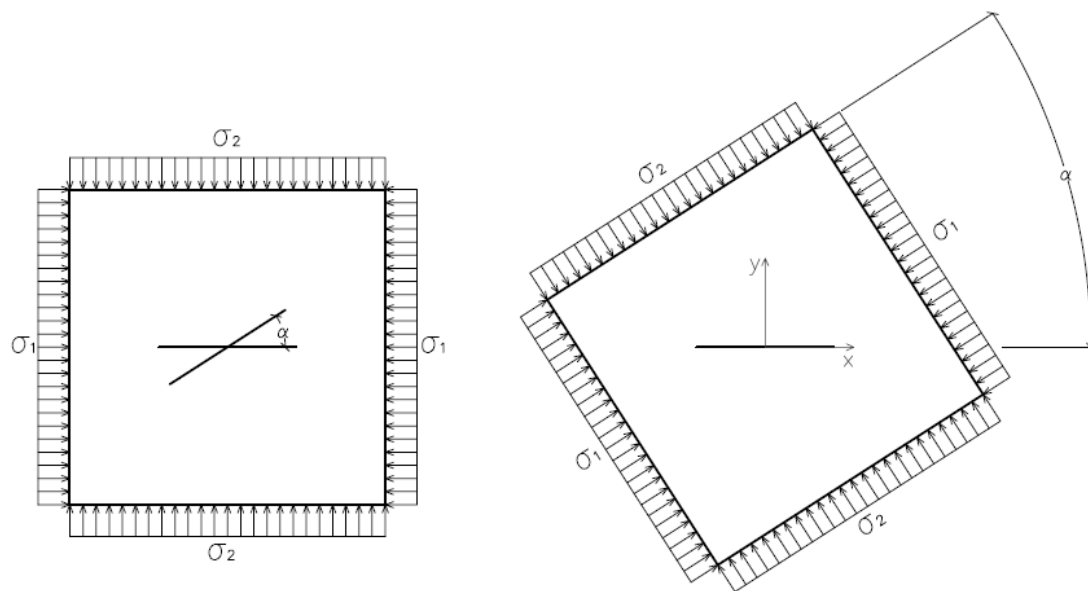


Figure 11. Crack rotation modelling in studied model.

4.2 Coordinate systems

In order to model the geometry and the loads, three different coordinate systems have been used (see Figure 12)

The first axis is Cartesian. It is located on the right crack tip, where the stress intensity factors (K_I and K_{II}) have been calculated. Since it is a symmetric geometry with central crack, it must be ensured that the stress intensity factors are equal at both crack-tips, so the crack-tip on the right is used for calculate results.

As the crack does not rotate or change location, the keypoints, nodes and lines belonging to the crack, are associated with this axis. It will then be used to define the path that ANSYS software needs to calculate K_I and K_{II} .

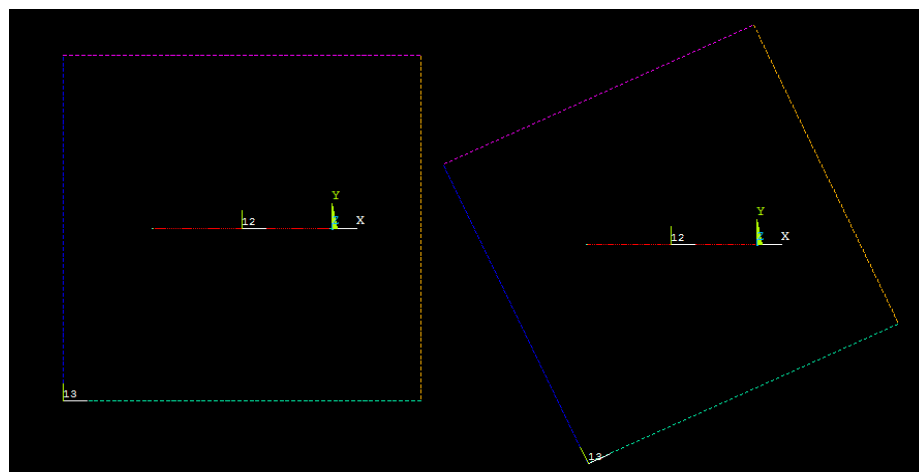


Figure 12. Coordinate system [8] in model

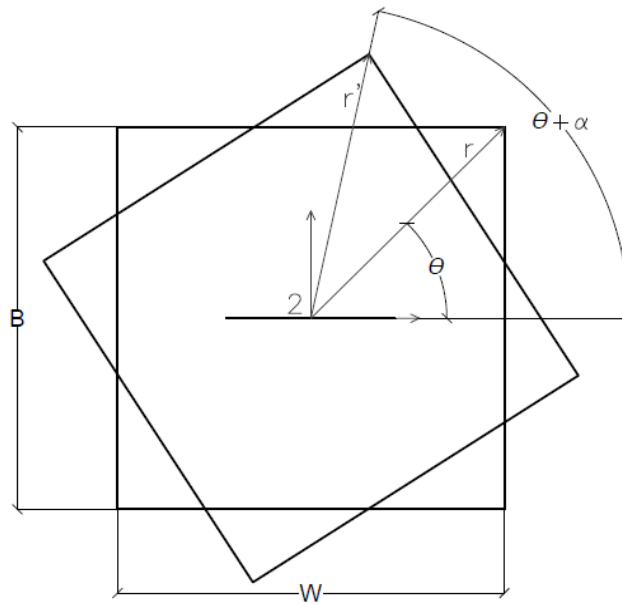


Figure 13. Polar coordinates on the model. Crack angle rotation

The second axis (number 12 on Figure 12) is in axis of polar coordinates. The polar coordinates serve to define the contour of the geometry and facilitate its rotation in each case.

Through the coordinates r and θ , the keypoints and lines of the contour of the geometry are defined. Thus, for a new different α angle, simply change the θ parameter in the model (see Figure 13).

To define the keypoints associated to this axis, basic concepts of trigonometry have been used in order to convert Cartesian coordinates into polar coordinates:

The third axis is Cartesian (number 13 on Figure 12). It is located on left bottom corner. It is used for maintain forces and supports perpendicular to the shape when the geometry is rotated. All peripheral nodes are rotated with this axis and also, forces and supports with them.

4.3 Element type

PLANE183 element type has been adopted to take into account crack singularity (see Figure 14). It is a 2-D, 8-node element. It has quadratic displacement behavior and is well suited to modeling irregular meshes. Each node has two degrees of freedom: translation in the nodal x and y directions. This element has plasticity, hyperelasticity, creep, stress stiffening, large deflection, and large strain capabilities [8].

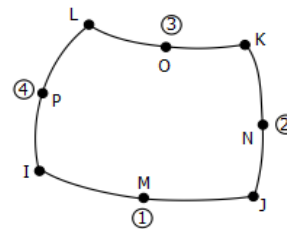


Figure 14. PLANE183 element type on ANSYS software [8]

4.4 Mesh

The results provided by ANSYS are based on the finite element method (FEM). This method allows to obtain an approximate solution on a continuous domain solving differential equation associated to a physical problem. The process of discretization is the first step of FEM and lies in dividing the domain in small subdomains formed by a mesh of points called nodes, in order to transform the equations in a system of algebraic equations.

First of all, **keypoints** are defined. In order to get better results near crack tip, we should create keypoints around the crack tip forming a circle (see Figure 15).

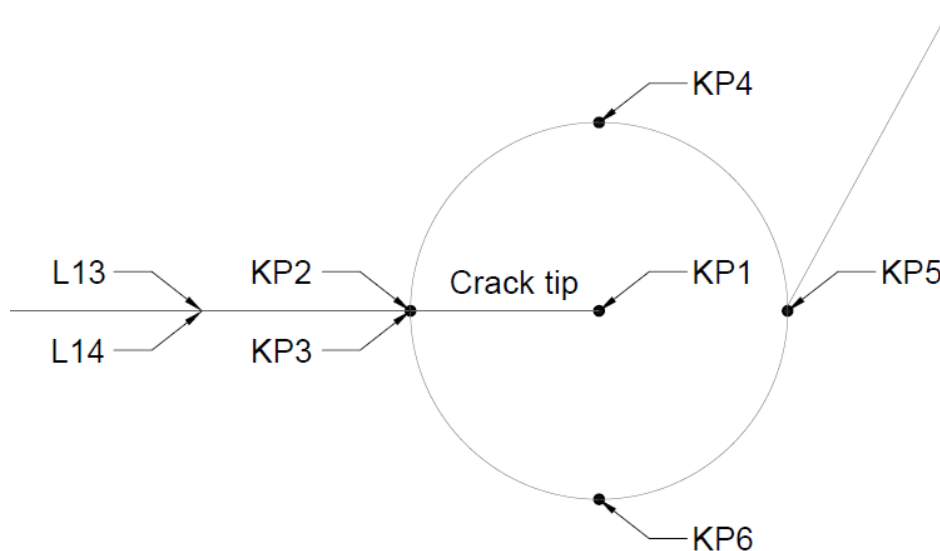


Figure 15. Distribution of keypoints and lines on right crack tip.

Like is shown in Figure 15 there are two coincident nodes (KP2 and KP3) on the crack tip. The same occurs on the left side of the crack (KP8 and KP10). The purpose of this nodes is to model the crack. Two lines (L13 and L14) are set between this four nodes. Thereby, when forces are applied, the crack could open (mode I) or slide (mode II).

The rest of the lines have two purposes (see Figure 16). First, is to form the shape of the specimen. Second, is to divide areas on the geometry. In order to model the crack, six areas are created. To do this, it is necessary to join the points of the corners of the geometry with the tip of the crack. These lines divide the geometry into two areas, necessary for the software to simulate the behavior of the crack. It has been done this way so that when rotating the piece, these lines always divide the areas without intervening in other parts of the geometry.

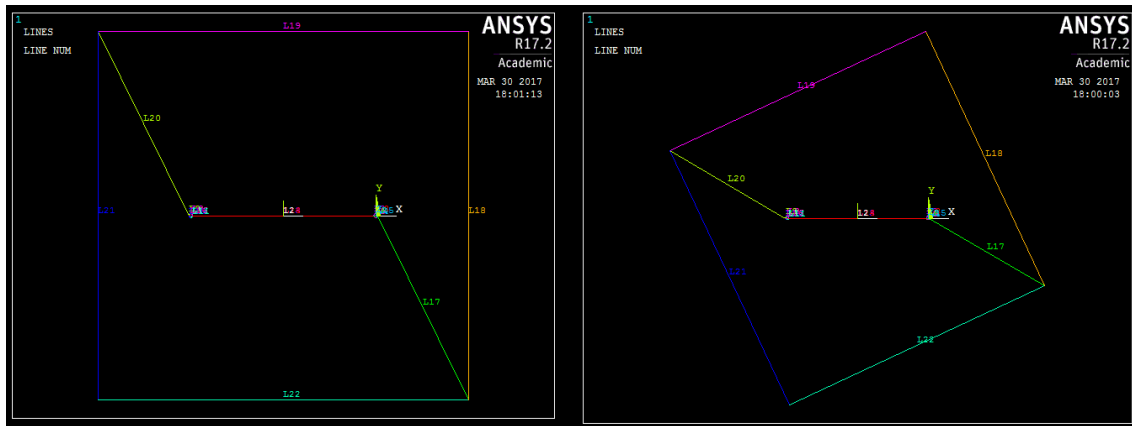


Figure 16. Modeling of specimen. Lines.

Next step is to create areas. As it is said, there are six areas on the geometry as is shown in the Figure 17 and Figure 18.

- Two areas in each half circle around crack tip.
- One area on the top and another on the bottom.

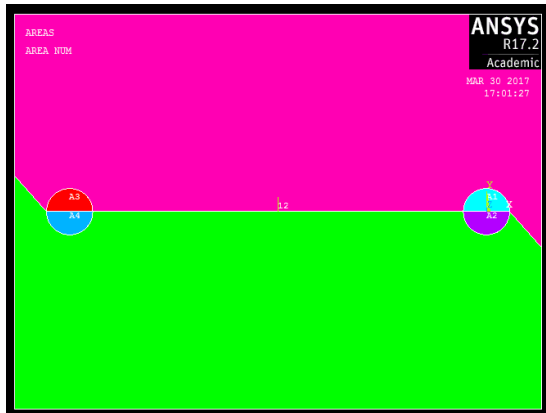


Figure 17. Detail of areas near crack tip

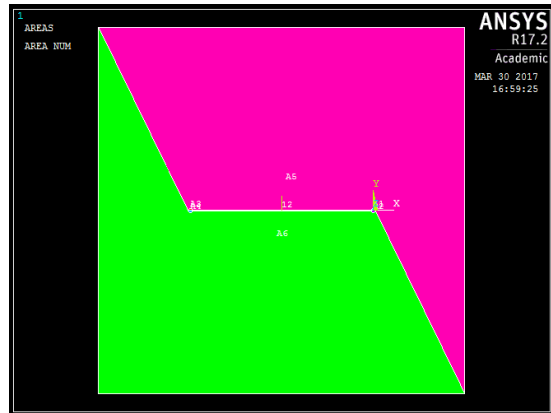


Figure 18. Creating areas on model

Last step is meshing the model. The mesh around the crack tip is generated with a special ANSYS command. This command (KSCON) is useful for modeling stress concentrations and crack tips. During meshing, elements are initially generated circumferentially about, and radially away, from the keypoint (See Figure 19). Lines attached to the keypoint are given appropriate divisions and spacing ratios [8]. Finally, nodes and area elements within areas are generated on the areas remaining (see Figure 20).

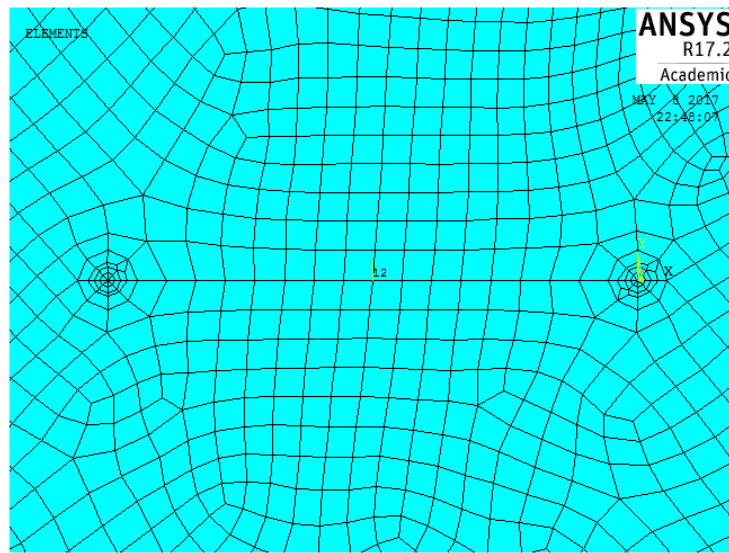


Figure 19. Detail of radial mesh around crack tip

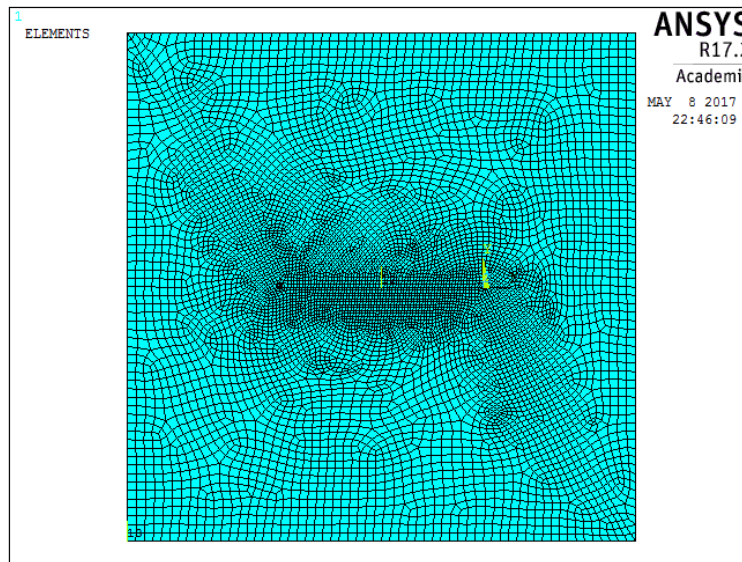


Figure 20 Creating model. Meshing.

4.5 Boundary conditions (Loads and supports)

In order to simulate mixed mode loading (I+II) conditions, supports and loads have been modeled on the specimen through the concept of action and reaction. The forces and supports are explained by the case of crack angle equal to zero. Subsequently and when rotating the piece, contour conditions will rotate therewith, always remaining perpendicular to the faces. In this way, the rotation of the crack is simulated and the mixed mode of loading can be observed (see Figure 21).

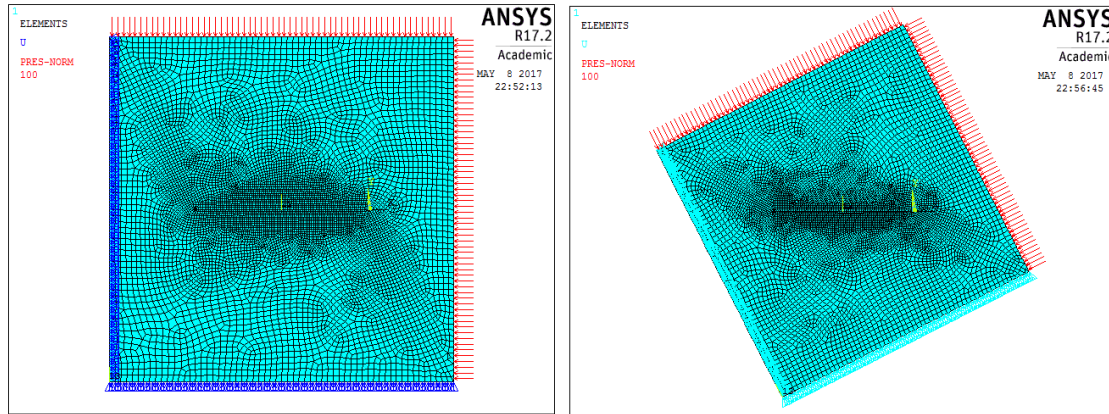


Figure 21 Boundary conditions for different angles (supports and loads)

Loads are applied as pressure, and as explained formerly, always perpendicular to the edges. A set of different biaxial loads (σ_2 and σ_1) have been applied to each crack length and angle. σ_2 has a constant value equal to 100 MPa, and is applied on the edge perpendicular to the notch when the crack angle (α) is 0°. σ_1 is applied parallel to the notch when crack angle (α) is 0° and it varies proportionally to σ_2 , according to the following equations:

$$\sigma_2 = 100$$

$$\sigma_1 = \frac{\sigma_1}{\sigma_2} \sigma_2$$

$$\frac{\sigma_1}{\sigma_2} = \{-1; -0.5; 0; 0.5; 1\}$$

On the other hand, and following the principle of action and reaction (see Figure 21), the stress has been applied only in one part of the geometry, whereas in the parallel faces simple supports have been applied as shown in the figure. These supports restrict movement in x and y so that the reactions on them are equal to the forces applied. It can be seen in Figure 19 that when rotating the geometry the supports rotate with it and remain perpendicular to the faces, as explained above when explaining axis number 13 (see Figure 12)

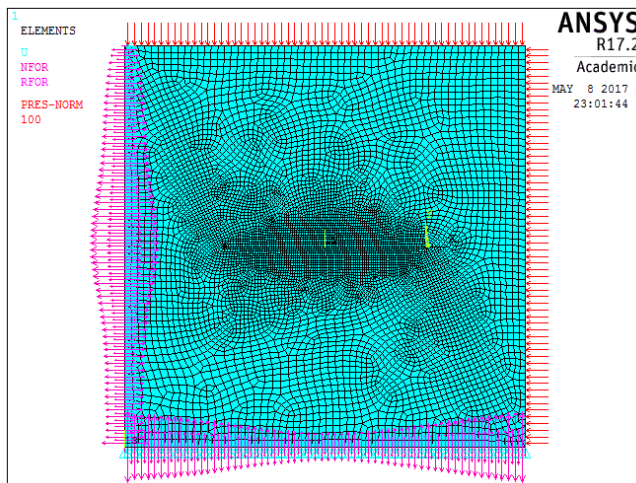


Figure 22. Principle of action and reaction. Forces on the top and right faces. Reactions on the left and bottom faces.

4.6 Material properties

As it is said all around this document, the extent of the zone evolving around the crack tip, where the material of a cracked body behaves in a macroscopically nonlinear manner, determines the fracture response [18].

The material used for our study is a concrete type which material properties are:

- Young's modulus; 40 GPa.
- Possion's ratio: $\nu = 0.2$.

Concrete is a quasi-brittle material and is englobed in a large group of materials used in engineering. As a material of these characteristics the process of fracture is specific. In general, the zone developed in the fracture is large (contrary to brittle materials). Therefore, the use of non-linear or multi-parametric fracture mechanics is necessary.

5 Results

In order to predict the angle of propagation of the crack under biaxial load, a lot of criteria have been explained on the theoretical part of this project. This section explains the results obtained thanks to the combination of different computer programs mentioned above, such as ANSYS and Wolfram Mathematica.

The table below summarizes the criteria explained above and the parameters used in each of them.

	K_I	K_{II}	T-stress	δ_I	δ_{II}	S_1	Approach
MTS	X	X					MTS Single-parametric approach.
	X	X	X				MTS Multi-parametric approach.
						X	Finite element method. Direct MTS
SED	X	X					SED Single-parametric approach.
	X	X	X				SED Multi-parametric approach.
CTOD	X	X					Finite element method (Single-parametric approach).
				X	X		Finite element method (Single-parametric approach).

Table 1. Comparison of different criteria

5.1 How to get each parameter

This is a very extensive analysis since each parameter has been obtained for different cases in which both the load, the length and the angle of the crack vary.

- Load cases : $\sigma_1/\sigma_2 = \{-1; -0.5; 0; 0.5; 1\}$
- Crack length: $a/W = \{0.1; 0.2; 0.3; 0.4; 0.5; 0.6; 0.7; 0.8; 0.9\}$
- Angle of crack: $\alpha = \{0^\circ; 9^\circ; 18^\circ; 27^\circ; 36^\circ; 45^\circ\}$

5.1.1 Stress intensity factor (K_I and K_{II})

These parameters indicate the mode of loading to which the geometry is subjected. As explained above, the ANSYS software is able to calculate them. The methodology was based on creating the model in the program as explained in the previous section and obtaining these parameters.

The following tables (Table 2. to Table 4.) are the values of K_I and K_{II} expressed in MPa \sqrt{m}



		Crack lenght 0.1			Crack lenght 0.2			Crack lenght 0.3		
		σ_1/σ_2	KI	KII	σ_1/σ_2	KI	KII	σ_1/σ_2	KI	KII
Angle of crack 0°	-1	534,62	0,629	-1	773,76	2,8495	-1	983,44	9,8623	
	-0,5	534,62	0,63626	-0,5	773,76	2,8554	-0,5	983,44	9,8694	
	0	534,61	0,70037	0	773,76	2,8613	0	983,43	9,8764	
	0,5	534,61	0,70449	0,5	773,75	2,8672	0,5	983,43	9,8834	
	1	534,61	0,7086	1	773,75	2,873	1	983,43	9,8904	
Angle of crack 9°	σ_1/σ_2	KI	KII	σ_1/σ_2	KI	KII	σ_1/σ_2	KI	KII	
	-1	508,36	167,21	-1	734,52	241,23	-1	930,4	307,63	
	-0,5	514,9	125,68	-0,5	744,07	182,35	-0,5	942,99	235,19	
	0	521,44	84,144	0	753,61	123,48	0	955,57	162,75	
	0,5	527,98	42,609	0,5	763,16	64,602	0,5	968,15	90,309	
Angle of crack 18°	1	534,52	1,0748	1	772,2	5,7276	1	980,73	17,87	
	σ_1/σ_2	KI	KII	σ_1/σ_2	KI	KII	σ_1/σ_2	KI	KII	
	-1	432,17	317,11	-1	623,48	455,3	-1	785,86	573,89	
	-0,5	457,66	238,1	-0,5	660,31	343,23	-0,5	833,16	435,92	
	0	483,16	159,08	0	697,15	231,17	0	880,45	297,96	
Angle of crack 27°	0,5	508,65	80,072	0,5	733,98	119,1	0,5	927,75	159,99	
	1	534,15	1,0605	1	770,81	7,0393	1	975,04	22,025	
	σ_1/σ_2	KI	KII	σ_1/σ_2	KI	KII	σ_1/σ_2	KI	KII	
	-1	313,81	436,7	-1	451,14	625,34	-1	564	783,24	
	-0,5	386,72	327,88	-0,5	530,33	470,82	-0,5	665,07	592,87	
Angle of crack 36°	0	423,63	219,07	0	609,53	316,3	0	766,13	402,51	
	0,5	478,55	110,25	0,5	688,72	161,78	0,5	867,2	212,14	
	1	533,46	1,4347	1	767,92	7,2645	1	968,27	21,775	
	σ_1/σ_2	KI	KII	σ_1/σ_2	KI	KII	σ_1/σ_2	KI	KII	
	-1	164,78	512,56	-1	235,1	733,38	-1	287,42	915,07	
Angle of crack 45°	-0,5	256,96	384,65	-0,5	367,83	551,38	-0,5	456,37	690,73	
	0	349,13	256,74	0	500,55	369,38	0	625,32	466,38	
	0,5	441,31	128,83	0,5	633,28	187,39	0,5	794,28	242,04	
	1	533,48	0,91769	1	766	5,3928	1	963,23	17,694	
	σ_1/σ_2	KI	KII	σ_1/σ_2	KI	KII	σ_1/σ_2	KI	KII	
Angle of crack 45°	-1	0,46635	538,79	-1	4,4092	769,59	-1	17,373	957,51	
	-0,5	133	404,2	-0,5	188,1	577,94	-0,5	227,23	720,93	
	0	266,46	269,62	0	380,62	386,29	0	471,84	484,35	
	0,5	399,93	135,04	0,5	573,13	194,64	0,5	716,44	247,78	
	1	533,4	0,45919	1	765,64	2,9909	1	961,05	11,199	

Table 2. Stress Intensity factor for various crack length ratios (I)



		Crack lenght 0,4			Crack lenght 0,5			Crack lenght 0,6		
Angle of crack 0°	σ_1/σ_2	KI	KII	σ_1/σ_2	KI	KII	σ_1/σ_2	KI	KII	
	-1	1194,2	24,535	-1	1423	48,08	-1	1689,2	79,596	
	-0,5	1194,1	24,543	-0,5	1423	48,088	-0,5	1689,2	76,605	
	0	1194,1	24,551	0	1423	48,097	0	1689,2	79,613	
	0,5	1194,1	24,559	0,5	1423	48,105	0,5	1689,2	79,622	
	1	1194,1	24,567	1	1423	48,113	1	1689,2	79,631	
Angle of crack 9°	σ_1/σ_2	KI	KII	σ_1/σ_2	KI	KII	σ_1/σ_2	KI	KII	
	-1	1123,7	378,97	-1	1330,2	461,65	-1	1568,5	561,26	
	-0,5	1140,1	294,61	-0,5	1351,7	365,91	-0,5	1697,4	453,57	
	0	1156,4	210,25	0	1373,2	270,18	0	1626,2	345,87	
	0,5	1172,8	125,89	0,5	1394,7	174,44	0,5	1655	238,18	
	1	1189,1	41,531	1	1416,2	78,701	1	1683,8	130,48	
Angle of crack 18°	σ_1/σ_2	KI	KII	σ_1/σ_2	KI	KII	σ_1/σ_2	KI	KII	
	-1	940,88	693,85	-1	1100,4	823,45	-1	1277,2	976,9	
	-0,5	1000	532,85	-0,5	1174,5	641,57	-0,5	1371,6	773,43	
	0	1059,2	372,23	0	1248,6	459,68	0	1466	569,95	
	0,5	1118,3	211,61	0,5	1322,6	277,8	0,5	1560,4	366,48	
	1	1177,4	50,983	1	1396,7	95,91	1	1654,8	163,01	
Angle of crack 27°	σ_1/σ_2	KI	KII	σ_1/σ_2	KI	KII	σ_1/σ_2	KI	KII	
	-1	665,23	936,14	-1	760,1	1098	-1	853,15	1279	
	-0,5	789,93	714,63	-0,5	913,3	847,74	-0,5	1043,6	1001,2	
	0	914,63	493,13	0	1066,5	579,52	0	1234	723,42	
	0,5	1039,3	271,62	0,5	1219,7	347,31	0,5	1424,4	445,61	
	1	1164	50,115	1	1372,9	97,098	1	1614,8	167,8	
Angle of crack 36°	σ_1/σ_2	KI	KII	σ_1/σ_2	KI	KII	σ_1/σ_2	KI	KII	
	-1	325,41	1085,3	-1	347,2	1257,9	-1	351,71	1439,87	
	-0,5	532,5	824,55	-0,5	598,4	964,43	-0,5	658,34	1117,3	
	0	739,59	563,81	0	849,6	671,01	0	946,97	794,76	
	0,5	946,69	303,07	0,5	1100,8	377,59	0,5	1271,6	472,23	
	1	1153,8	42,321	1	1352	84,717	1	1578,2	149,7	
Angle of crack 45°	σ_1/σ_2	KI	KII	σ_1/σ_2	KI	KII	σ_1/σ_2	KI	KII	
	-1	45,415	1127,8	-1	94,592	1290,1	-1	172,48	1451,9	
	-0,5	253,18	853,31	-0,5	265,22	983,46	-0,5	260,03	1118,8	
	0	551,77	578,79	0	625,04	676,82	0	692,53	785,66	
	0,5	850,36	304,28	0,5	984,85	370,18	0,5	1125	452,52	
	1	1148,9	29,761	1	1344,7	63,541	1	1557,5	119,38	

Table 3. Stress Intensity Factor for different crack length ratios (II)



	Crack lenght 0,7			Crack lenght 0,8			Crack lenght 0,9		
	σ_1/σ_2	KI	KII	σ_1/σ_2	KI	KII	σ_1/σ_2	KI	KII
Angle of crack 0°	-1	2027,3	118,94	-1	2536,9	158,78	-1	3608,2	204,13
	-0,5	2027,3	118,85	-0,5	2537	158,79	-0,5	3608,2	204,14
	0	2027,3	118,86	0	2536,9	158,8	0	3608,2	204,15
	0,5	2027,3	118,87	0,5	2536,9	158,81	0,5	3608,2	204,16
	1	2027,3	118,08	1	2536,9	158,82	1	3608,2	204,17
Angle of crack 9°	-1	1871,8	687	-1	2322,8	865,36	-1	3219,1	1198,6
	-0,5	1911,7	565,75	-0,5	2381,2	724,01	-0,5	3315,4	1021,9
	0	1951,6	443,92	0	2439,7	582,65	0	3411,7	845,11
	0,5	1991,5	322,1	0,5	2498,1	441,3	0,5	3508,1	668,35
	1	2031,4	200,27	1	2556,5	299,95	1	3604,4	491,6
Angle of crack 18°	-1	1492,7	1169,8	-1	1794,1	1434,4	-1	2315,3	1879,1
	-0,5	1616,8	942,38	-0,5	1965	1177,1	-0,5	2573,3	1575,6
	0	1740,9	714,96	0	2135,9	919,7	0	2831,2	1272,2
	0,5	1865	487,54	0,5	2306,8	662,35	0,5	3089,2	968,74
	1	1989	260,12	1	2477,7	404,99	1	3347,2	665,3
Angle of crack 27°	-1	953,34	1498,7	-1	1076,9	1786,4	-1	1256,7	2204,8
	-0,5	1194,5	1192,7	-0,5	1391,9	1449,7	-0,5	1691,8	1831,2
	0	1435,7	886,67	0	1707	1113	0	2126,9	1457,6
	0,5	1676,9	580,66	0,5	2022	776,25	0,5	2562	1084
	1	1918,1	274,64	1	2337	439,54	1	2997,2	710,41
Angle of crack 36°	-1	334,55	1647,3	-1	295,66	1897,1	-1	231,57	2225,2
	-0,5	712,87	1297,7	-0,5	769,88	1522,3	-0,5	841,45	1826,9
	0	1091,2	948,07	0	1244,1	1147,4	0	1451,3	1428,7
	0,5	1469,5	598,45	0,5	1718,3	772,64	0,5	2061,2	1030,4
	1	1847,8	248,84	1	2192,5	397,84	1	2671,1	632,18
Angle of crack 45°	-1	285,54	1617,7	-1	444,36	1794,6	-1	665,8	1993,2
	-0,5	236,37	1264,4	-0,5	190,18	1428,4	-0,5	114,53	1623,3
	0	758,28	911,09	0	824,72	1062,3	0	894,87	1253,4
	0,5	1280,2	557,78	0,5	1459,3	696,1	0,5	1675,2	883,41
	1	1802,1	204,47	1	2093,8	329,93	1	2455,5	513,47

Table 4. Stress Intensity Factor for different crack length ratios (III)

When K_I is big, mode I predominates and the same occurs for mode II. The following images (Figure 23,

Figure 24 and Figure 25) show the stress fields in the vicinity of the crack tip for ratio $a / W = 0.5$ and inclination angle of 45° .

For ratio of load $\sigma_1 / \sigma_2 = -1$, K_{II} is much bigger than K_I so the predominant mode is mode II. There is a different situation in each case.

	σ_1/σ_2	KI	KII
Ratio crack	0,5	-1	94,592
Angle of crack	45°	-0,5	265,22
		0	625,04
		0,5	984,85
		1	1344,7
			63,541

Table 5. Stress Intensity Factor for crack length ratio $a/W=0.5$

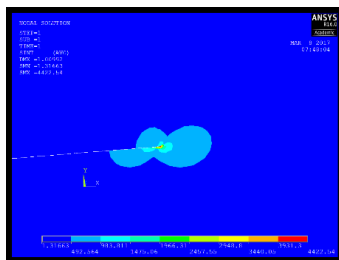


Figure 23. Dominant Mode II
 $\sigma_1/\sigma_2 = -1$

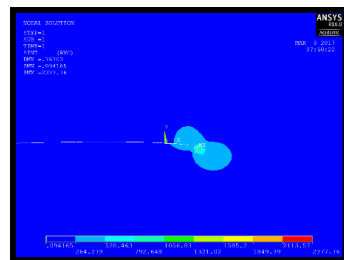


Figure 24. Almost equal Mode I
and II
 $\sigma_1/\sigma_2 = 0$

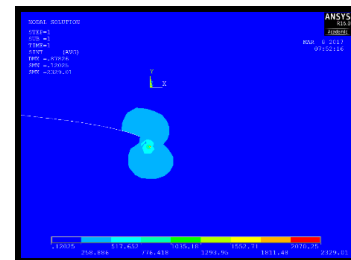


Figure 25. Dominant Mode I
 $\sigma_1/\sigma_2 = 1$

5.1.2 T-stress

For T-stress calculation σ_{xx} and σ_{yy} values have been used. To obtain them ANSYS software has been used. As this parameter represents the stress parallel to the crack line the methodology in ANSYS has been:

- 1.- Create a PATH near the crack tip. This path is parallel to the x axis and is defined in Cartesian coordinates. (Figure 26)



Figure 26. Selected nodes as path used for calculation of T-stress.

- 2.- Calculate the σ_{xx} and σ_{yy} values for each node on that path on ANSYS. (Figure 27)

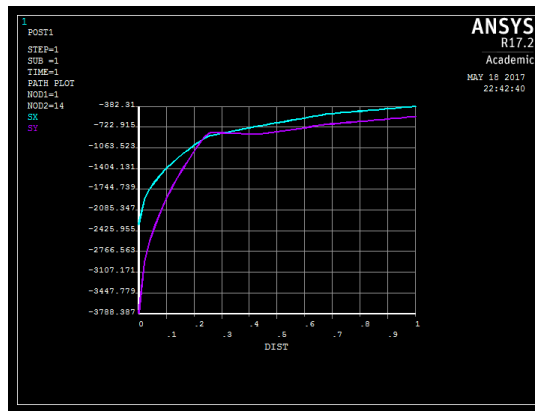


Figure 27. σ_{xx} and σ_{yy} for a specific geometry and load case

- 3.- Following the equation (18), calculate T-stress for each node.

$$T = (\sigma_{xx} - \sigma_{yy})_{\theta=0} \quad (18)$$

- 4.- Using a linear regression, calculate T-stress in the vicinity of the crack tip.

Steps 3 and 4 have been done with Excel.

Figure 28 show the steps for one of the different cases. This procedure has been repeated for each case of geometry and load.

Graph 1. to Graph 10. show the evolution of T-stress for the different situations.

$\sigma_1/\sigma_2 = -1$				
Ratio of crack length 0.1				
Angle of crack 0°				
S	SX	SY	sx-sy	sx-sy
0	-755,12	-1422,5	667,38	
2,00E-02	-602,89	-1108,3	505,41	
4,00E-02	-539,83	-978,14	438,31	
6,00E-02	-491,45	-878,28	386,83	
8,00E-02	-450,65	-794,09	343,44	
0,1	-414,71	-719,92	305,21	
0,12	-382,22	-652,87	270,65	
0,14	-352,34	-591,2	238,86	
0,16	-324,53	-533,81	209,28	
0,18	-298,41	-479,9	181,49	
0,2	-273,71	-428,92	155,21	
0,22	-250,21	-380,42	130,21	
0,24	-227,76	-334,09	106,33	
0,26	-213,65	-312,43	98,78	
0,28	-207,19	-314,01	106,82	
0,3	-200,72	-315,58	114,86	
0,32	-194,26	-317,16	122,9	
0,34	-187,8	-318,73	130,93	
0,36	-181,34	-320,31	138,97	
0,38	-174,87	-321,88	147,01	
0,4	-168,41	-323,46	155,05	
0,42	-161,95	-325,03	163,08	
0,44	-155,56	-325,81	170,25	
0,46	-149,72	-320,96	171,24	171,24
0,48	-143,87	-316,12	172,25	172,25
0,5	-138,02	-311,27	173,25	173,25
0,52	-132,18	-306,42	174,24	174,24
0,54	-126,33	-301,57	175,24	175,24
0,56	-120,49	-296,72	176,23	176,23
0,58	-114,64	-291,88	177,24	177,24
0,6	-108,79	-287,03	178,24	178,24
0,62	-102,95	-282,18	179,23	179,23
0,64	-97	-277,33	180,23	180,23
0,66	-91	-272,48	181,226	181,226
0,68	-85	-267,64	182,233	182,233
0,7	-82	-264,46	182,204	182,204
0,72	-79	-261,44	182,071	182,071
0,74	-76	-258,43	181,948	181,948
0,76	-74	-255,41	181,815	181,815
0,78	-71	-252,39	181,682	181,682
0,8	-68	-249,38	181,559	181,559
0,82	-65	-246,36	181,426	181,426
0,84	-62	-243,34	181,293	181,293
0,86	-59	-240,33	181,17	181,17
0,88	-56	-237,31	181,038	181,038
0,9	-53	-234,3	180,915	180,915
0,92	-50	-231,28	180,782	180,782
0,94	-48	-228,26	180,649	180,649
0,96	-45	-225,25	180,526	180,526
0,98	-42	-222,23	180,393	180,393
1	-39	-219,22	180,27	180,27

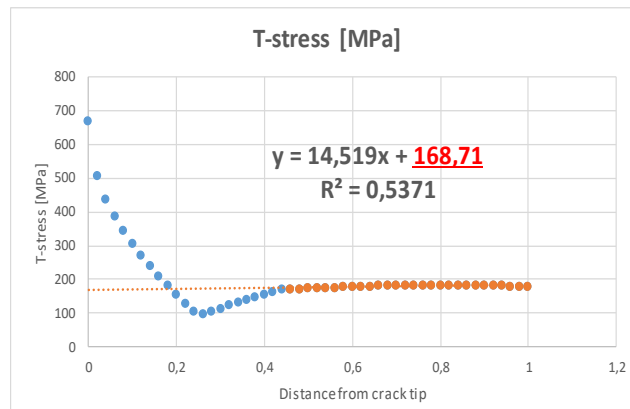
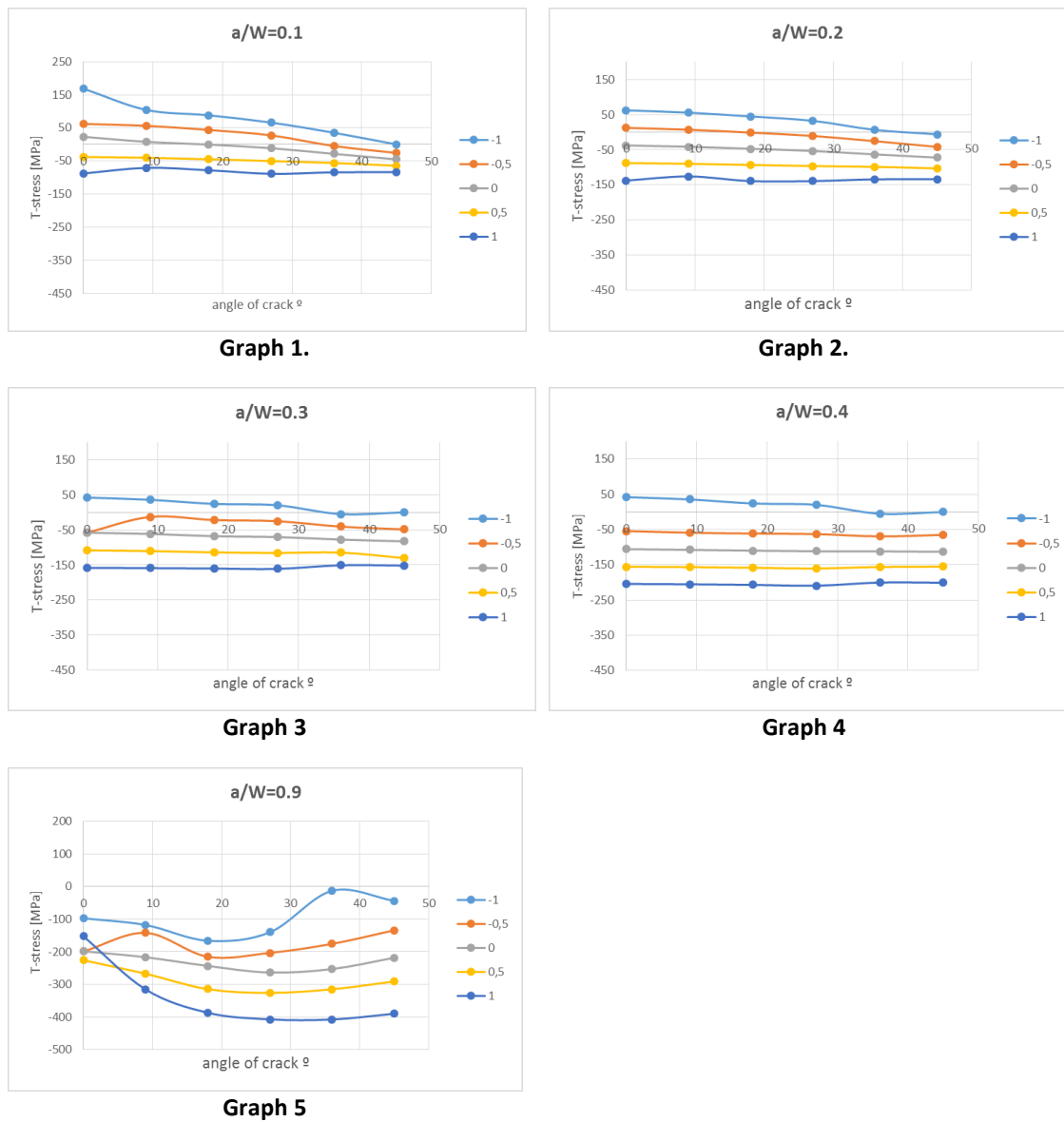
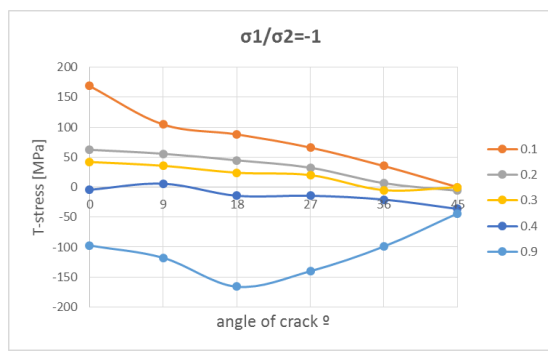
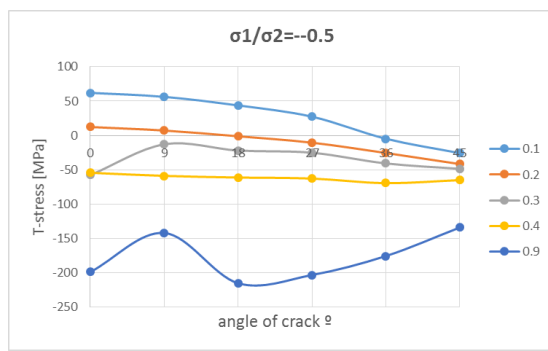
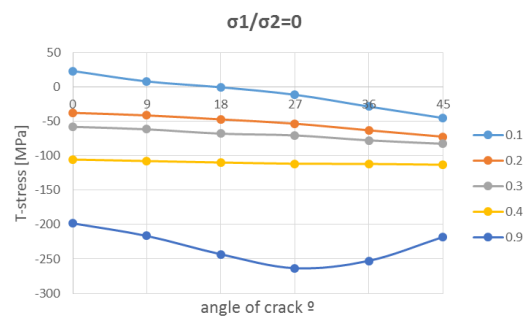
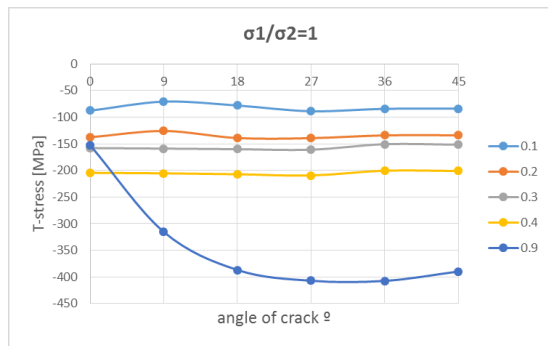


Figure 28. Calculation of T-stress in Excel.



Graph 1, Graph 2, Graph 3, Graph 4 and Graph 5. Evolution of T-stress for different length ratios. Each colour shows the evolution for a different load ratio.


Graph 6.

Graph 7.

Graph 8.

Graph 9.

Graph 10.

Graph 6, Graph 7, Graph 8, Graph 9 and Graph 10. Show the evolution of T-stress for different load ratios. Each colour shows the evolution for a different length ratio.

5.1.3 Displacements (δ_I and δ_{II})

The displacements have been obtained with ANSYS software following this steps:

- 1.- Select two coincident nodes from both faces of the crack, near the crack tip. (See Figure 29. **Displacement of two coincident nodes from both faces of the crack**)
- 2.- Obtain displacement in x and y direction for each node. With a simple command in ANSYS the displacements can be obtained.
- 3.- Calculate the variation of displacement in each direction for each node, using cartesian coordinates. It has been done with Excel. (Table 6)

This procedure has been repeated for each case of geometry and load.

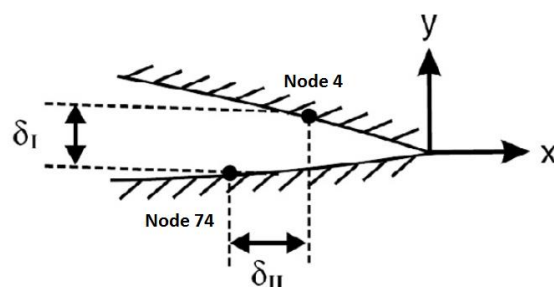


Figure 29. Displacement of two coincident nodes from both faces of the crack [3]

σ_1/σ_2	Node	Ratio of crack lenght 0.1				
		Displacement in x and y direction obtained from ANSYS		Variation of displacement in x and y direction.		
		X(A/C)	Y(B/D)	δ_x	δ_y	
Angle of crack 0°	-1	Node 4	0,41664703	-0,37868299	2,5493E-05	-0,02711583
		Node 74	0,41662154	-0,35156716		
	-0,5	Node 4	0,25864116	-0,35268381	2,5702E-05	-0,03711569
		Node 74	0,25861546	-0,31556812		
	0	Node 4	0,10063529	-0,30668463	2,5909E-05	-0,02711556
		Node 74	0,10060939	-0,27956908		
	0,5	Node 4	-0,05737057	-0,27068545	2,6117E-05	-0,02711542
		Node 74	-0,05739669	-0,24357003		
	1	Node 4	-0,21837644	-0,23468627	-0,00297367	-0,02711528
		Node 74	-0,21540277	-0,20757099		

Table 6. Values of displacements in x and y direction obtained in ANSYS

5.1.4 Principal Tensile Stress S_1

This parameter has been calculated on ANSYS and Excel.

1.- Create a radial path around the crack-tip using polar coordinates. (Figure 30)



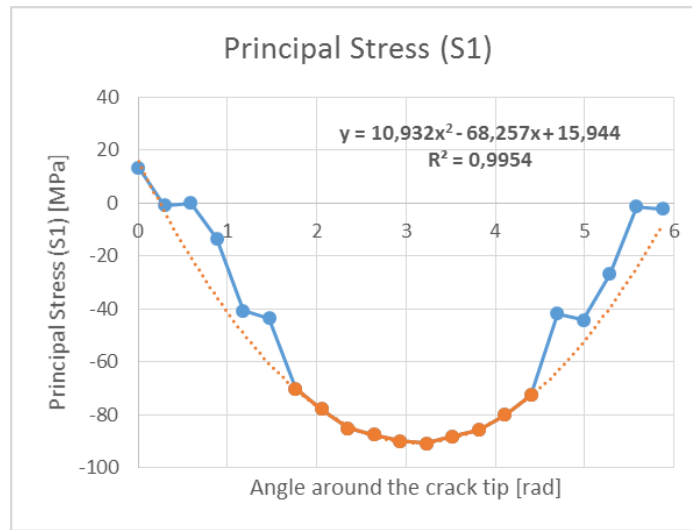
Figure 30. Path for calculation of Principal Tensile Stress

2.-Obtain the principal Stress S_1 for each node on this path with ANSYS command.

3.- Approximate the results to a polynomial regression with Excel. The equation will be used later for calculate the angle of propagation (θ). (Table 7 and Graph 11)

Ratio of crack length 0.1					
angle of crack 0°	$\sigma_1/\sigma_2=1$				
	$S (\sigma)$		S	S_1	
	0		0	13	
	16,8140195		0,29346	-1	
	33,6280389		0,58692	0	
	50,4420584		0,88038	-13	
	67,253786		1,1738	-41	
	84,0700973		1,4673	-43	
	100,886409		1,7608	-70	-70
	117,69699		2,0542	-78	-78
	134,513302		2,3477	-85	-85
	151,323883		2,6411	-88	-88
	168,140195		2,9346	-90	-90
	184,956506		3,2281	-91	-91
	201,767088		3,5215	-88	-88
	218,583399		3,8150	-86	-86
	235,39971		4,1085	-80	-80
	252,210292		4,4019	-73	-73
	269,026603		4,6954	-42	
	285,837185		4,9888	-44	
	302,653496		5,2823	-27	
	319,469807		5,5758	-1	
	336,280389		5,8692	-2	

Table 7. Values of Principal Tensile Stress for an specific geometry



Graph 11. Evolution of Principal Tensile Stress and equation from results on Table 7

5.2 How to obtain angle of propagation θ

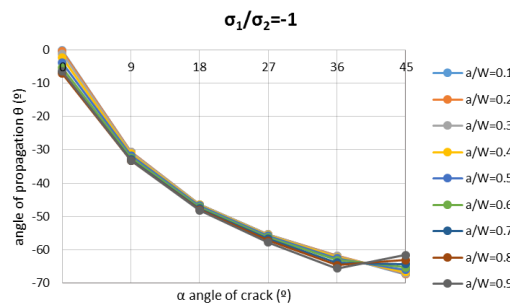
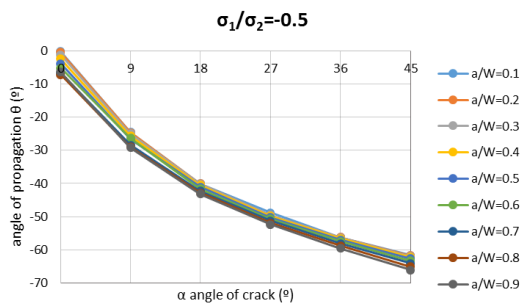
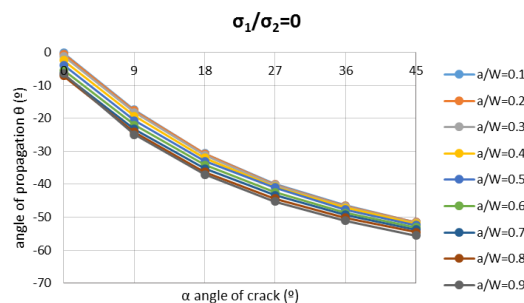
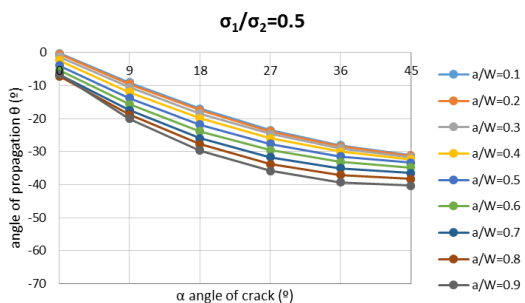
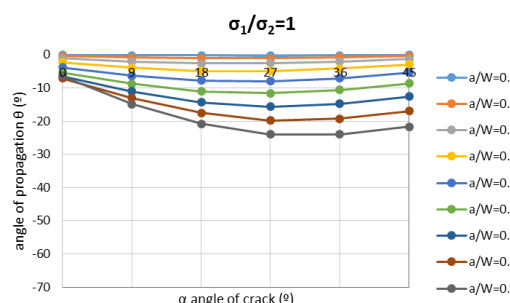
For each criterion and approach the equations mentioned throughout this document have been used. All data previously obtained have been used in both Excel and Wolfram Mathematica for the calculation of the propagation angle.

5.2.1 MTS Single-parametric approach.

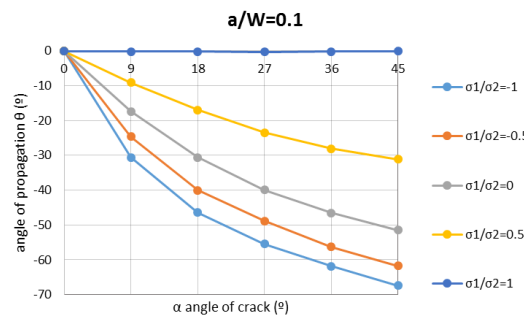
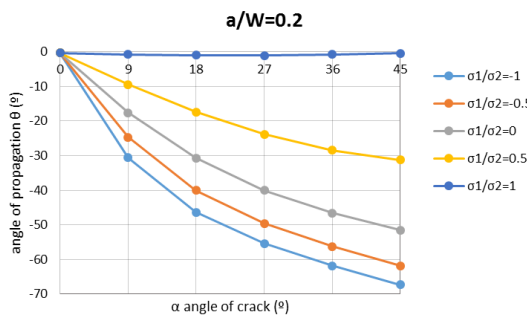
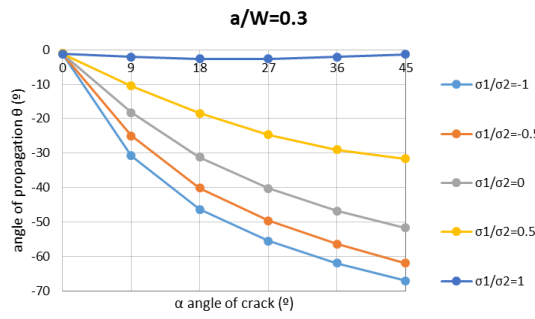
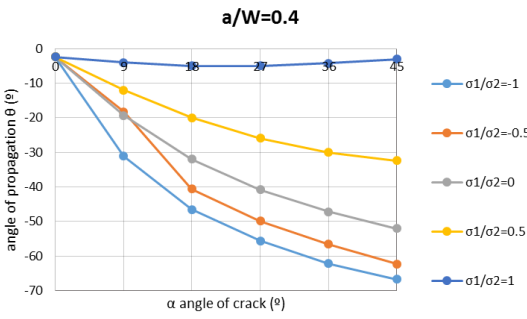
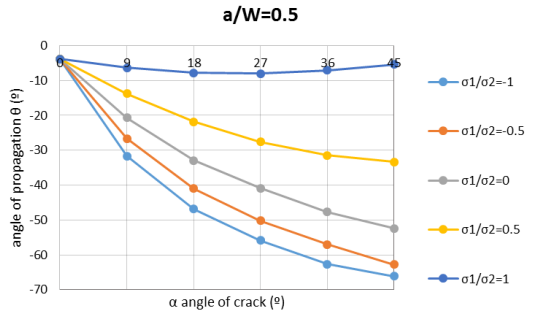
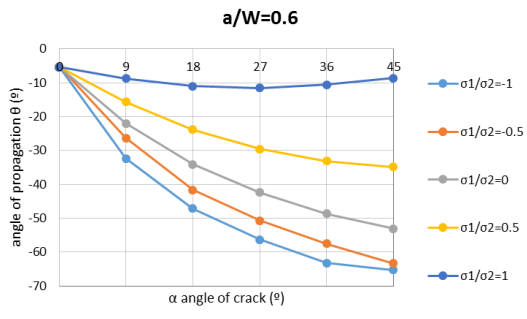
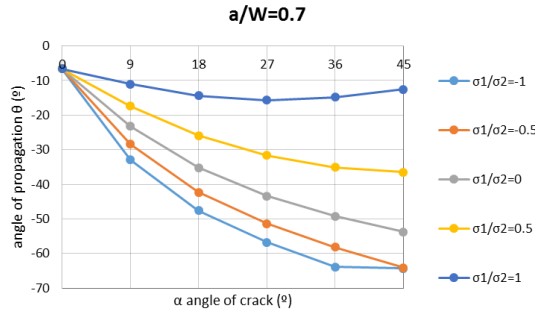
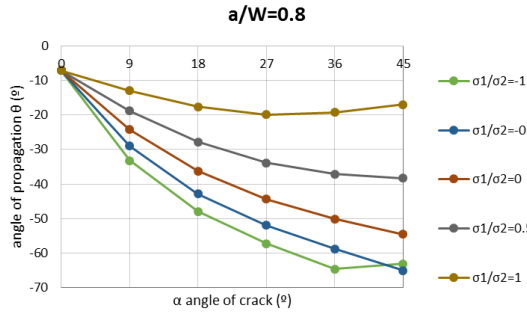
	K_I	K_{II}	T-stress	δ_I	δ_{II}	S_1	Approach
MTS	X	X					MTS Single-parametric approach.

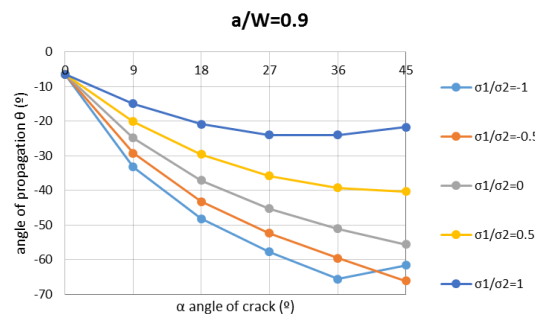
Applying equation ((25) for θ the following results have been obtained:

$$\theta = \begin{cases} 2 \operatorname{arctg} \frac{1}{4} \left(\frac{K_I}{K_{II}} + \sqrt{\left(\frac{K_I}{K_{II}} \right)^2 + 8} \right) & \text{for } K_{II} < 0 \\ 0 & \text{for } K_{II} = 0 \\ 2 \operatorname{arctg} \frac{1}{4} \left(\frac{K_I}{K_{II}} - \sqrt{\left(\frac{K_I}{K_{II}} \right)^2 + 8} \right) & \text{for } K_{II} > 0 \end{cases} \quad (25)$$


Graph 12.

Graph 13.

Graph 14.

Graph 15.

Graph 16.

Graph 12, Graph 13, Graph 14, Graph 15 and Graph 16. Initiation angle θ for various crack angle α and ratio a/W . MTS criterion


Graph 17.

Graph 18.

Graph 19.

Graph 20.

Graph 21.

Graph 22.

Graph 23.

Graph 24.


Graph 25

Graph 17, Graph 18, Graph 19, Graph 20, Graph 21, Graph 22, Graph 23, Graph 24 and Graph 25.
Comparison of influence of the stress ratio σ_1/σ_2 on initiation angle θ for various crack angle α and length ratio a/W .

5.2.2 MTS Multi-parametric approach.

	K_I	K_{II}	T-stress	δ_I	δ_{II}	S_1	Approach
MTS	X	X	X				MTS Multi-parametric approach.

To obtain the angle of propagation, the equation ((27) have been used. AS the equation is complex, the numerical calculation have been done in Wolfram Mathematica.

$$[K_I \sin \theta + K_{II}(3 \cos \theta - 1)] - \frac{16 T}{3} \sqrt{2\pi r} \cos \theta \sin \frac{\theta}{2} = 0 \quad (27)$$

The following images show an example of the methodology. (Figure 31)

Crack lenght 0.1				
Angle of crack 0°	σ_1/σ_2	K_I	K_{II}	T-STRESS
	-1	534,62	0,629	168,71
	-0,5	534,62	0,63626	62,07
	0	534,61	0,70037	23,161
	0,5	534,61	0,70449	-37,932
	1	534,61	0,7086	-87,782

Table 8. Values of Stress Intensity factor and T-stress for $a/W=0.1$ and crack inclination angle $\alpha=0^\circ$

```
In[7]:= Solve[(534.62 Sin[\theta] + 0.629 (3 Cos[\theta] - 1)) - (16 + 168.71)/3 Sqrt[2 \[Pi] r] Cos[\theta] Sin[\theta/2] == 0, \theta]
[seno] [resuelve]
Out[7]= {{\theta \[Rule] -4.42529}, {\theta \[Rule] -1.16367}, {\theta \[Rule] 0.00212108}, {\theta \[Rule] 1.16343}, {\theta \[Rule] 4.42417}, {\theta \[Rule] 6.28243}}
```

... **Solve:** Inverse functions are being used by Solve, so some solutions may not be found; use Reduce for complete solution information.

Assuming a list of rules | Use as a two-dimensional array or a list instead
apply rules to variable | apply rules to expr... | first solution | convert rules to lists | | |

Figure 31. Calculation of angle of propagation (θ) in Wolfram Mathematica. MTS with T-stress approach

It can be seen in the Figure 31 that the software obtains several results. It have had to choose the correct value for the MTS approach.

5.2.3 Direct MTS criterion.

	K_I	K_{II}	T-stress	δ_I	δ_{II}	S_1	Approach
MTS						X	Finite element method. Direct MTS.

Once the polynomial expression of Principal Tensile Stress (S_1) is obtained, the assumption is that the angle will propagate in the direction of maximum tensile stress (S_1).

The procedure is to derive the polynomial expression (Equation (41)) and equate to zero. Then, solve the unknown which is the angle of propagation (θ).

This procedure has been done in Excel obtaining the polynomial expression of S_1 as explained in the section below (see Graph 11 and Table 7). The following equations (41) are an example. In this case, the values of a and b are the ones on the Table 9 bellow. Following the next equations (41) the angle of propagation can be calculated:

Crack lenght 0.1					
Angle of crack 0°	σ_1/σ_2	a	b	θ (rad)	θ (deg)
	-1	10,932	-68,257	3,12189	1,12888665
	-0,5	23,267	-146,45	3,147161	-0,31905509
	0	54,657	-336,32	3,076642	3,72142117
	0,5	64,072	-399,96	3,121176	1,16977795
	1	67,071	-418,53	3,120052	1,23419511

Table 9. Values of polynomial regression a and b . Angle of propagation (θ) calculated in means of MTS.

$$S_1 = a\theta^2 + b\theta + c \rightarrow S_1 = 10.932 \theta^2 + 68.257 \theta + 15.944$$

$$\frac{\delta S_1}{\delta \theta} = 0 \quad (41)$$

$$2a\theta + b = 0 \rightarrow 2 \times 10.932 \theta - 68.257 = 0$$

$$\theta = -\frac{b}{2a} \rightarrow \theta = -\frac{10.932}{2 \times (-68.257)} = 0.32032 [rad]$$

5.2.4 SED Single-parametric approach.

	K_I	K_{II}	T-stress	δ_I	δ_{II}	S_1	Approach
SED	X	X					SED Single-parametric approach.

The angle was obtained with equation (31) and the stress intensity factors.

$$\theta = \arctg \left(\frac{2 K_I K_{II}}{K_I^2 + K_{II}^2} \right) \quad (31)$$

5.2.5 SED Multi-parametric approach.

	K_I	K_{II}	T-stress	δ_I	δ_{II}	S_1	Approach
SED	X	X	X				SED Multi-parametric approach.

As in MTS Multi-Parametric approach and due to the complexity of the equation (32) the angle have been obtained with Wolfram Mathematica. The following image is an example:

$$\begin{aligned} \frac{\delta S}{\delta \theta} = & \frac{K_I^2}{16 \mu \pi r} [(\kappa - \cos \theta)(1 + \cos \theta)] + \frac{K_I K_{II}}{8 \mu \pi r} \sin \theta [(1 - \kappa) + 2 \cos \theta] \\ & + \frac{K_{II}^2}{16 \mu \pi r} [(1 + \kappa)(1 - \cos \theta) + (1 + \cos \theta)(3 \cos \theta - 1)] \\ & + \frac{K_I T}{4 \mu \sqrt{2 \pi r}} \cos \frac{\theta}{2} [(\kappa - 2) - \cos \theta + 2(\cos \theta)^2] \\ & - \frac{K_{II} T}{4 \mu \sqrt{2 \pi r}} \sin \frac{\theta}{2} [\kappa + \cos \theta + 2(\sin \theta)^2] + \frac{1 + \kappa}{16 \mu} T^2 \end{aligned} \quad (32)$$

```
In[190]:= A = 313.81
B = 436.7
T = 66.027

Out[190]= 313.81
Out[191]= 436.7
Out[192]= 66.027

In[193]:= Solve[(A^2/(837.758)*((3.5 - Cos[x])*(1 + Cos[x])) + (A+B)/(418.879)*Sin[x]*(-2.5 + 2*Cos[x]) + (B^2/(837.758)*(4.5*(1 - Cos[x]) + (1 - Cos[x))*(3*Cos[x] - 1)) + (A+T)/(167.1085)*Cos[x/2]*(1.5 - Cos[x] + 2*Cos[x]^2) - (B+T)/(167.1085)*Sin[x/2]*(3.5 + Cos[x] + 2*Cos[x]^2) + 0.016875*T == 0), x]
(* Solve: Inverse functions are being used by Solve, so some solutions may not be found; use Reduce for complete solution information. *)
Out[193]= {{x -> -3.92042 - 0.419866 I}, {x -> -3.92042 + 0.419866 I}, {x -> -0.699433 - 3.13346 I}, {x -> -0.699433 + 3.13346 I}, {x -> 0.34667 - 1.17456 I}, {x -> 0.34667 + 1.17456 I}, {x -> 1.67246}, {x -> 3.49197}, {x -> 6.07876 - 0.437467 I}, {x -> 6.07876 + 0.437467 I}}
```

Figure 32. Calculation of angle of propagation (θ) in Wolfram Mathematica. SED with T-stress approach.

Where A is K_I , B is K_{II} and T is T-stress for a specific geometry in Figure 32.

As in MTS criterion, the correct value of the angle (x in the Figure 32) has been analysed and chosen from the different results given by Wolfram Mathematica.

5.2.6 CTD

	K_I	K_{II}	T-stress	δ_I	δ_{II}	S_1	Approach
CTOD	X	X					Finite element method (Single-parametric approach).
				X	X		Finite element method (Single-parametric approach).

The methodology is easy for CTOD criterion. Once all the parameters were obtained (K_I , K_{II} , and δ_I , δ_{II}) is just necessary to apply equations (33) and (34) respectively.

$$tg \theta = \frac{\delta_{II}}{\delta_I} \quad (33)$$

$$tg \theta = \frac{K_{II}}{K_I} \quad (34)$$

6 Discussion

The objective of this thesis has been to analyze the different existing criteria for the calculation of the propagation angle (θ) for materials that do not follow the mechanics of linear elastic fracture. Given that the results obtained have not been expected in many ways, as they differ widely from each other, this conclusion will try to explain possible calculation errors as well as the causes of these discrepancies. Due to the big amount of results is a complicate to analyze them. As the results have been obtained by different methods, software and with different criteria, there are big differences between them.

It can be seen that the angles obtained with each method are very different one from each other. The explanation of this fact could be done because of different causes.

First of all, it is necessary to emphasize the possible errors that have been able to produce in the calculation. These errors may have occurred throughout the procedure, and may be due to both human errors and because of the software used.

- Results given by Wolfram Mathematica (MTS with T-stress and SED with T-stress) are quite ambiguous since the software provided different results for each equation so it has had to choose a result between all the options.
- The finite element method can lead to errors when the mesh is not suitable. This has caused problems in ANSYS, especially when the inclination of the crack is big or when the crack length ratio is too big or too small.
- The calculation of the angles has been done using the parameters (K_I , K_{II} , T-stress) so there may be some previous mistakes in the calculation of them.
 - o The stress intensity factors have been calculated in ANSYS, so errors can be attributed to problems when meshing the geometry.
 - o The calculation of T-stress has been done through ANSYS as well as Excel. The value has been approximated with linear regression that already carries errors. Moreover, T-stress can have negative values in ANSYS although K_I and K_{II} have been calculated on ANSYS following the equations (38), (39) and (40) with absolute value of nodal displacement.
- The calculation of principal tensile stress (S_1) is also problematic due to the data obtained from ANSYS have been approximated by polynomial regression that also carries errors.

From other point of view, the big differences can be caused by the different approach of each criterion. It can be observed that the values generally follow a coherent distribution within the same criterion but when comparing with other criterion they are not consequent. Some of the reason to explain this discrepancy are the ones that follow:

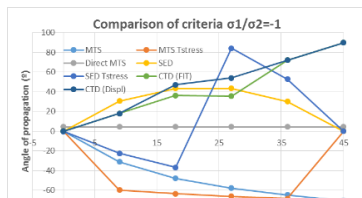
- As each criterion is based on different assumptions, the results are different. The MTS criterion is based on tangential stress while the SED criterion on strain energy and CTD on displacements.
- It can be seen that for the different approaches of CTD criterion (displacements and stress intensity factors) the angles obtained are very similar, so it can be said that these are two coherent criteria among themselves.

- The results obtained for the MTS and SED criteria with the single-parametric approach (that means without the T-stress parameter) are comparable and similar up to an angle of 18° or 27° generally. The solution is sometimes stable only for first angles of crack inclination. Generally for 0°, 9° and 18° is stable, while when the angle is bigger the criteria fails.
- The greater divergence of results can be observed when the direct method of the MTS criterion is applied. There is no way to compare these results with the other criteria, so it must be an error in both the theoretical part and the calculation procedure.
- When comparing MTS without T-stress and with T-stress, it can be observed that the values are quite similar for ratio crack $a/W=0.1$ and $a/W=0.2$. From there, the values of MTS with T-stress tend to 70° for all applied length and forces.
- Other parameter which cause big errors is the ratio of load applied. It can be found some errors when the ratio applied is $\sigma_1/\sigma_2 = 1$.
- T-stress is also difficult to calculate with the method used and it has been not possible to approximate the value when the angle of inclination is 45° in some cases, and the ratio of load the one mentioned above.
- The addition of the T-stress parameter in the Williams expansion is one of the major causes of these differences. It can be seen the big influence of this parameter that has been explained on theoretical background. This study showed the differences between the criteria with and without T-stress.

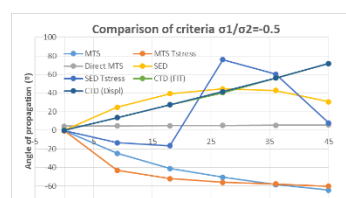
As a sample of the results, tables and graphs for the ratios $a/W= 0.1; 0.2; 0.3; 0.4; 0.9$ are provided on the following pages. (Graph 26 to Graph 50, Table 10 to Table 14)

Ratio crack 0,1												
				MTS	MTS Tstress	Direct MTS	SED	SED Tstress	CTD (FIT)	CTD (Displ)		
	σ_1/σ_2	KI	KII	T-STRESS	$\Theta(\text{deg})$							
Angle of crack 0°	-1	534,62	0,629	168,71	-0,13482073	0,12152893	1,12888665	0,13482073	-0,26913812	0,06741055	0,05386672	
	-0,5	534,62	0,63626	62,07	-0,13637684	-0,60885933	-0,31905509	0,13637684	-0,270857	0,06818861	0,03967637	
	0	5,35E+02	7,00E-01	23,161	-0,15012096	-0,67023457	3,72142117	0,15012096	-0,28403503	0,07506074	0,05474628	
	0,5	534,61	0,70449	-37,932	-0,15100406	-0,10242652	1,16977795	0,15100406	-0,30007785	0,07550229	0,05518692	
	1	534,61	0,7086	-87,782	-0,15188501	0,07241041	1,23419511	0,15188501	-0,28632686	0,07594277	6,25849289	
Angle of crack 90°				MTS	MTS Tstress	Direct MTS	SED	SED Tstress	CTD (FIT)	CTD (Displ)		
	-1	508,36	167,21	104,54	-31,0780819	-59,5784434	1,41944893	30,6941367	-22,3612448	18,2070927	18,1410556	
	-0,5	514,9	125,68	56,271	-24,8560976	-43,0554865	7,21359418	24,7366318	-13,3526294	13,7168998	13,6605298	
	0	5,21E+02	8,41E+01	8,001	-17,4804728	-19,1577606	14,829682	17,4607764	-3,14996992	9,16671366	9,11400701	
	0,5	527,98	42,609	-40,276	-9,1109279	-6,09300508	6,28925541	9,1103568	-12,3849037	4,61388036	4,57957256	
Angle of crack 18°	1	534,52	1,0748	-70,866	-0,23041579	-0,12215976	26,2017406	0,23041579	-0,36539503	0,11520882	0,09300354	
				MTS	MTS Tstress	Direct MTS	SED	SED Tstress	CTD (FIT)	CTD (Displ)		
	-1	432,17	317,11	88,089	-47,9015686	-63,3794454	1,4029406	43,649164	-36,788895	36,2698127	47,2810591	
	-0,5	457,66	238,1	43,811	-41,051873	-51,9416035	15,6067078	39,3130334	-16,4689468	27,4859406	27,4159947	
	0	4,83E+02	1,59E+02	-0,4707	-31,0997102	-30,9746714	30,0616099	30,7143491	-2,02525377	18,2240835	18,172718	
Angle of crack 27°	0,5	508,65	80,072	-44,746	-17,0960036	-11,1660307	45,5999986	17,078411	-25,9852028	8,94612073	1,039E-08	
	1	534,15	1,0605	-78,055	-0,22750769	-0,11558449	75,7234124	0,22750769	-0,36253024	0,11375474	0,10712362	
				MTS	MTS Tstress	Direct MTS	SED	SED Tstress	CTD (FIT)	CTD (Displ)		
	-1	313,81	436,7	66,027	-57,6147532	-66,1783442	1,14926497	43,4641856	84,1751006	35,7007974	54,2385956	
	-0,5	386,72	327,88	27,343	-50,4651808	-55,8689427	25,1698111	44,6115499	75,8695044	40,2928973	41,5577195	
Angle of crack 36°	0	4,24E+02	2,19E+02	-11,383	-40,9241693	-37,9224149	48,4903736	39,2154658	64,7793333	27,3446508	27,263978	
	0,5	478,55	110,25	-50,103	-23,7254092	-15,0625448	175,930496	23,6314746	49,3810926	12,973629	78,5751434	
	1	533,46	1,4347	-88,821	-0,30818006	0,14585557	2522,58416	0,30818006	39,8253025	0,15409226	0,12933137	
				MTS	MTS Tstress	Direct MTS	SED	SED Tstress	CTD (FIT)	CTD (Displ)		
	-1	164,78	512,56	35,288	-64,5275021	-68,3280819	1,6210856	30,2311121	52,9133774	72,2431277	72,1241153	
Angle of crack 45°	-0,5	256,96	384,65	-4,746	-58,4586333	-57,6172088	32,2544448	42,7318738	60,4025087	56,2556553	56,1947157	
	0	3,49E+02	2,57E+02	-28,537	-47,9419571	-40,6257447	123,126228	43,6679044	66,507374	36,3296768	36,2484041	
	0,5	441,31	128,83	-56,229	-28,524939	-17,3668091	208,078013	28,2804046	54,6586068	16,2739139	16,2227871	
	1	533,48	0,91769	-84,285	-0,19711855	-0,09587245	-84,8480089	0,19711855	38,2777435	0,09855986	0,54850576	
				MTS	MTS Tstress	Direct MTS	SED	SED Tstress	CTD (FIT)	CTD (Displ)		
Angle of crack 45°	-1	0,46635	538,79	??	-70,5122494	0	1,3548987	0,09918462	0	89,9504076	89,9552762	
	-0,5	133	404,2	-25,728	-64,390216	-60,0511335	34,9927186	30,7018006	7,83936059	71,7864666	71,736686	
	0	2,66E+02	2,70E+02	-45,112	-53,3095001	-41,4708571	1121,70164	44,9980092	18,0454578	45,3377342	45,2546761	
	0,5	399,93	135,04	-64,499	-31,6470345	-17,8932428	-66,952439	31,2243601	25,4721367	18,6577215	18,6021379	
	1	533,4	0,45919	-83,884	-0,09864868	-0,04809328	-57,8688513	0,09864868	37,9820972	0,04932441	0,0382216	

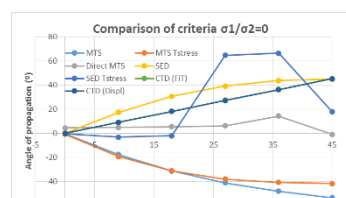
Table 10. Comparison of the angle of propagation for $a/W= 0.1$ for different criteria



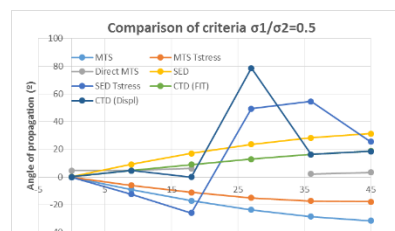
Graph 26.



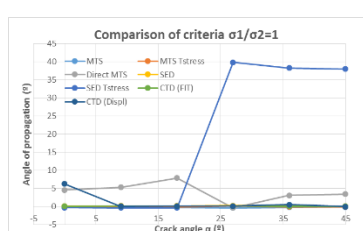
Graph 27.



Graph 28.



Graph 29.

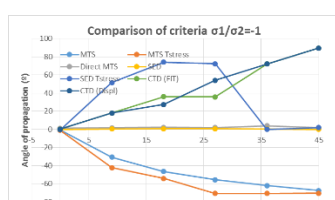


Graph 30.

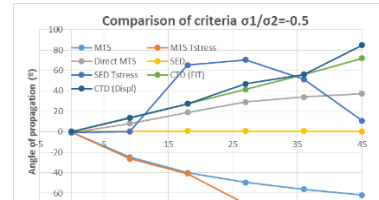
Graph 26, Graph 27, Graph 28, Graph 29 and Graph 30. Comparison of the angle of propagation for $a/W= 0.1$ for different criteria

Ratio crack 0,2											
				MTS	MTS Tstress	Direct MTS	SED	SED Tstress	CTD (FIT)	CTD (Displ)	
	σ_1/σ_2	KI	KII	T-STRESS	$\Theta(\text{deg})$	$\Theta(\text{deg})$	$\Theta(\text{deg})$	$\Theta(\text{deg})$	$\Theta(\text{deg})$	$\Theta(\text{deg})$	
Angle of crack 0°	-1	773,76	2,8495	62,313	-0,42198771	-0,91379893	1,28987423	0,0073651	-0,50806152	0,21100029	0,19710977
	-0,5	773,76	2,8554	12,309	-0,42286139	-0,47317261	-0,71616016	0,00738035	-0,48113251	0,21143717	0,19754557
	0	7,74E+02	2,86E+00	-37,688	-0,42373507	-0,31952195	-0,05428266	0,0073956	-0,52525026	0,21187405	0,19797845
	0,5	773,75	2,8672	-87,689	-0,42461423	-0,24160656	4,35591843	0,00741094	-0,51952068	0,21231368	0,19841397
	1	773,75	2,873	-137,69	-0,42547312	-0,19433124	1,20312511	0,00742593	-0,52123955	0,21274316	0,20871721
Angle of crack 9°	-1	734,52	241,23	55,733	-30,5656078	-42,0906255	1,67897754	0,53517432	51,7886612	18,18114	18,1304551
	-0,5	744,07	182,35	7,1836	-24,6724658	-26,168243	8,12633634	0,43309478	0,1812067	13,7701398	13,7158732
	0	7,54E+02	1,23E+02	-41,366	-17,6208775	-13,3713452	18,1391202	0,30891788	38,2932133	9,30530359	9,26109781
	0,5	763,16	64,602	-89,921	-9,52669472	-5,40617192	22,8909817	0,16653982	7,33458477	4,83859038	4,92054641
	1	772,2	5,7276	-125,92	-0,84983341	-0,40666997	27,5073307	0,01483259	39,4838196	0,42496929	0,40367709
Angle of crack 18°	-1	623,48	455,3	44,846	-46,3929638	-54,1193588	2,2800682	0,76109866	74,2296992	36,1390109	27,4159947
	-0,5	660,31	343,23	-1,1477	-40,0489119	-40,8356761	18,9808652	0,68589616	65,4038573	27,4654697	27,3877604
	0	6,97E+02	2,31E+02	-47,149	-30,765366	-40,430837	33,904992	0,53875153	55,1771336	18,3451552	77,7661767
	0,5	733,98	119,1	-93,149	-17,4700277	-70,312347	50,879121	0,30625778	45,8041171	9,21682357	64,5535846
	1	770,81	7,0393	-139,15	-1,04626385	-66,3089786	85,8952145	0,01826113	42,4904156	0,52323007	0,50767899
Angle of crack 27°	-1	451,14	625,34	32,459	-55,4307471	-70,5041756	2,11944221	0,75921723	72,4145689	35,8078688	54,108717
	-0,5	530,33	470,82	-10,479	-49,5748916	-70,4858409	29,3005181	0,78186487	70,4539073	41,5982475	46,8928971
	0	6,10E+02	3,16E+02	-53,414	-6,0153028	-70,4537553	55,3305197	0,68542029	63,4758543	27,4259009	29,2591786
	0,5	688,72	161,78	-96,351	-23,8623907	-70,3655198	145,743631	0,41888189	51,9806021	13,2190955	13,1622725
	1	767,92	7,2645	-139,29	-1,08378218	-66,4367482	-3431,96307	0,01891599	42,6494114	0,54200018	0,51653088
Angle of crack 36°	-1	235,1	733,38	6,6917	-61,8621145	-70,5047485	3,96498091	0,52662613	implex numbt	72,2256818	72,1708596
	-0,5	367,83	551,38	-25,527	-56,2672132	-70,4875598	34,1038879	0,74554624	51,5520297	56,2924306	56,2126682
	0	5,01E+02	3,69E+02	-63,056	-46,5729694	-70,4594849	107,030323	0,76266679	63,6190938	36,4254062	36,3448847
	0,5	633,28	187,39	-98,589	-28,4189849	-70,3832815	-241,487464	0,49834959	55,7264283	16,4836892	16,4361266
	1	766	5,3928	-134,11	-0,80664524	-65,026699	-89,59978	0,01407879	41,488026	0,40336759	0,39724621
Angle of crack 45°	-1	4,4092	769,59	-5,9053	-67,279168	-70,4130753	1,70319466	0,01145769	2,01768848	89,6717398	89,6796479
	-0,5	188,1	577,94	-41,642	-61,7801675	-70,4755277	37,3055869	0,5319837	10,807282	71,9716765	84,7773223
	0	3,81E+02	3,86E+02	-72,279	-51,5372311	-70,4537553	406,675866	0,7853435	20,799093	45,4235975	45,3411403
	0,5	573,13	194,64	-103,1	-31,2622995	-70,3821356	-75,2253234	0,54699723	58,2309987	18,7579401	18,7447579
	1	765,64	2,9909	-133,93	-0,44762341	-60,330164	-63,0255595	0,00781253	41,2800423	0,22381939	0,20871721

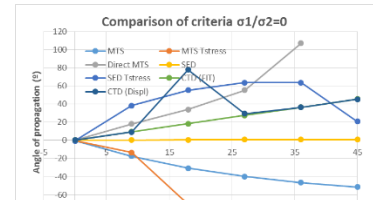
Table 11. Comparison of the angle of propagation for $a/W= 0.2$ for different criteria



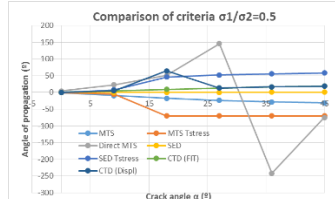
Graph 31.



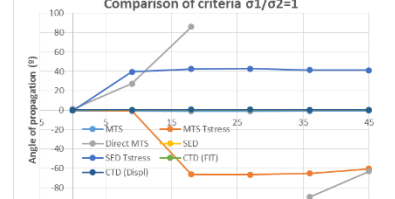
Graph 32.



Graph 33.



Graph 34.

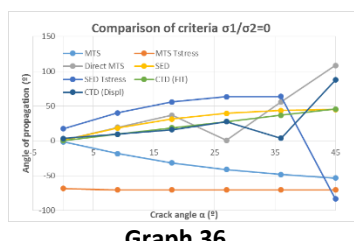


Graph 35.

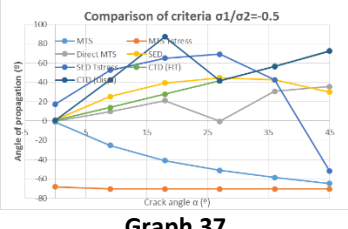
Graph 31, Graph 32, Graph 33, Graph 34 and Graph 35. Comparison of the angle of propagation for $a/W= 0.2$ for different criteria

Ratio crack 0,3											
				MTS	MTS Tstress	Direct MTS	SED	SED Tstress	CTD (FIT)	CTD (Displ)	
	σ_1/σ_2	KI	KII	T-STRESS	θ (deg)						
Angle of crack 0°	-1	983,44	9,8623	42,018	-1,14889699	-68,8437439	1,37165408	1,14889696	1,17185073	0,574564	0,55485911
	-0,5	983,44	9,8694	-57,695	-1,1497237	-68,271359	-0,2698584	1,14972368	17,4679163	0,57497761	0,55526914
	0	9,83E+02	9,88E+00	-57,981	-1,15055047	-68,299434	0,58837776	1,15055045	17,5424009	0,57539125	3,63750317
	0,5	983,43	9,8834	-107,98	-1,15136555	-67,9768587	11,5657348	1,15136553	29,5126351	0,57579903	0,55608988
	1	983,43	9,8904	-157,98	-1,15218063	-67,6777748	1,49224618	1,15218061	39,2156754	0,57620682	0,55650038
Angle of crack 9°	-1	930,4	307,63	35,694	-31,1912021	-70,4824032	2,73699831	30,79982	39,2156754	18,296093	18,2312298
	-0,5	942,99	235,19	-12,931	-25,285569	-70,444588	9,81377793	25,1550258	52,7678461	14,0043581	42,4108922
	0	9,56E+02	1,63E+02	-61,601	-18,3413383	-70,3907299	19,6194576	18,3161873	40,0825605	9,66570773	9,64845606
	0,5	968,15	90,309	-110,25	-10,4799712	-70,2509282	25,7114201	10,4784842	37,9941294	5,3291276	5,29564855
	1	980,73	17,87	-158,89	-2,08637147	-68,964065	32,8409852	2,08637101	39,9754174	1,04387782	1,02190583
Angle of crack 18°	-1	785,86	573,89	24,095	-47,8134231	-70,498446	3,22831573	43,6079084	72,3337818	36,1395356	88,141912
	-0,5	833,16	435,92	-21,931	-41,1716794	-70,4818302	21,1676746	39,4041427	65,0085164	27,6191414	87,1861711
	0	8,80E+02	2,98E+02	-67,951	-31,6958405	-70,4508905	36,6953155	31,2696968	55,8297326	18,6967371	16,032665
	0,5	927,75	159,99	-113,98	-18,54427	-70,3689575	55,4097367	18,5176699	46,1971661	9,7843924	16,0231112
	1	975,04	22,025	-160	-2,58541276	-69,2602842	94,7926971	2,58541142	40,6039521	1,29402381	1,27657903
Angle of crack 27°	-1	564	783,24	20,144	-57,5900246	-70,5070404	1,37165408	43,4830517	68,9550497	35,7571246	54,1581086
	-0,5	665,07	592,87	-25,147	-51,3048274	-70,4932894	-0,2698584	44,8112549	69,1733466	41,7150884	41,6250767
	0	7,66E+02	4,03E+02	-70,436	-41,2598568	-70,4692251	0,58837776	39,4702526	63,5228369	27,7165745	27,6404286
	0,5	867,2	212,14	-115,72	-24,8999291	-70,4056268	1,31759871	24,7793694	52,157646	13,7461045	13,699173
	1	968,27	21,775	-161,01	-2,57396511	-69,23622	1,49224618	2,5739638	40,9591859	1,28828255	1,27381463
Angle of crack 36°	-1	287,42	915,07	-4,9376	-64,6618458	-70,5070404	3,57371656	29,7601607	???	72,5626949	72,5060369
	-0,5	456,37	690,73	-40,702	-58,5818942	-70,4944353	30,7689352	42,6097957	42,5903968	56,5469896	56,4645441
	0	6,25E+02	4,66E+02	-77,649	-48,2012241	-70,4738088	55,9465866	43,785724	63,6878487	36,7165381	3,76918992
	0,5	794,28	242,04	-114,6	-29,4355593	-70,4188049	155,960591	29,1472002	55,8889391	16,9474892	16,8915318
	1	963,23	17,694	-150,65	-2,10332836	-68,9657839	-1332,14299	2,10332788	39,0294641	1,05237328	1,034357
Angle of crack 45°	-1	17,373	957,51	???	-70,1826304	???	3,34830931	2,07754667	???	88,9605431	88,9708684
	-0,5	227,23	720,93	-48,595	-64,6419425	-70,4869868	35,6722717	29,8305828	-51,9814439	72,5056644	72,4496122
	0	4,72E+02	4,84E+02	-82,66	-53,5263155	-70,4703711	108,414029	44,9901927	-83,4316703	45,7495679	87,4732566
	0,5	716,44	247,78	-130,32	-32,168865	-70,4130753	-253,027867	31,7078416	-52,3573042	19,0778889	18,9913159
	1	961,05	11,199	-151,69	-1,33489881	-68,0324356	-88,3133866	1,33489876	-1,44484752	0,66763061	2,44100128

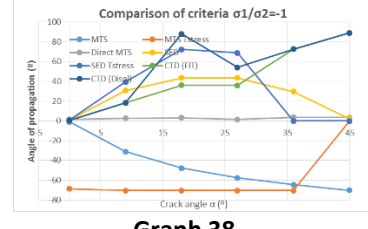
Table 12 Comparison of the angle of propagation for $a/W= 0.3$ for different criteria



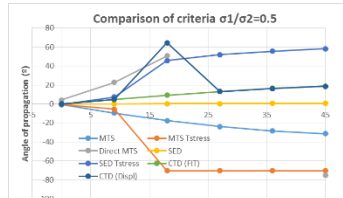
Graph 36.



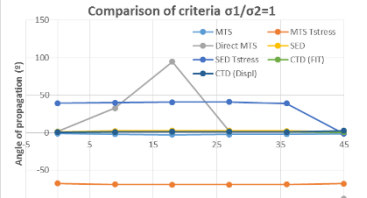
Graph 37.



Graph 38.



Graph 39.

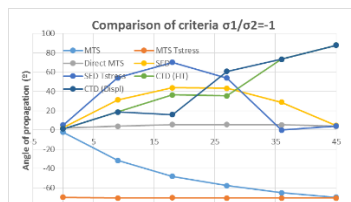


Graph 40.

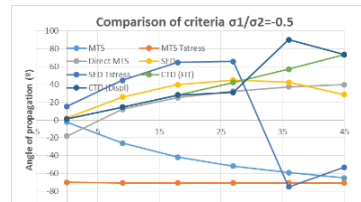
Graph 36, Graph 37, Graph 38, Graph 39 and Graph 40 Comparison of the angle of propagation for $a/W= 0.3$ for different criteria

Ratio crack 0,4											
				MTS	MTS Tstress	Direct MTS	SED	SED Tstress	CTD (FIT)	CTD (Displ)	
	σ_1/σ_2	KI	KII	T-STRESS	$\Theta(\text{deg})$	$\Theta(\text{deg})$	$\Theta(\text{deg})$	$\Theta(\text{deg})$	$\Theta(\text{deg})$	$\Theta(\text{deg})$	
Angle of crack 0°	-1	1194,2	24,535	-4,3868	-2,35198454	-69,7444335	1,79896029	2,3519837	5,16307473	1,17698393	1,15463008
	-0,5	1194,1	24,543	-54,38	-2,35294657	-69,6527603	-17,9087959	2,35294573	5,3880795	1,17746617	1,15501299
	0	1,19E+03	2,46E+01	-105,54	-2,35371203	-69,5582222	2,1848945	2,35371119	25,7391351	1,17784986	1,15539341
	0,5	1194,1	24,559	-155,54	-2,35447748	-69,465976	2,27442123	2,35447664	34,4320507	1,17823356	1,15577344
	1	1194,1	24,567	-204,38	-2,35524293	-69,3748758	1,20312511	2,35524209	41,6570485	1,17861726	1,15615427
Angle of crack 9°	-1	1123,7	378,97	5,81	-31,6208062	-70,4789654	3,83397343	31,1999863	54,0495527	18,6367782	18,5619293
	-0,5	1140,1	294,61	-58,88	-25,9993588	-70,4549012	12,1748815	25,8485434	44,5928843	14,4886987	14,4232005
	0	1,16E+03	2,10E+02	-107,71	-19,4254052	-70,4147941	21,3950651	19,3917054	48,085635	10,3046285	9,93644038
	0,5	1172,8	125,89	-156,54	-11,9854233	-70,321402	27,3870732	11,9825013	42,0902046	6,12675019	10,6515387
	1	1189,1	41,531	-205,36	-3,99094092	-69,8475659	27,5073307	3,99092915	42,7399388	2,00032307	1,96602929
Angle of crack 18°	-1	940,88	693,85	-14,332	-47,9939112	-70,2440527	5,61186134	43,6918592	70,1697203	36,4068418	15,9875699
	-0,5	1000	532,85	-61,262	-41,5561765	-70,4869868	25,0199677	39,6936991	64,4905626	28,0509223	27,9519813
	0	1,06E+03	3,72E+02	-109,87	-32,5179958	-70,4629226	39,5178205	32,0297176	57,086229	19,362781	19,2798114
	0,5	1118,3	211,61	-158,49	-20,1108671	-70,403335	57,7698229	20,0706405	49,1685252	10,7150882	10,6515387
	1	1177,4	50,983	-207,1	-4,94043578	-69,9707519	85,8952145	4,94040154	43,7328746	2,47943526	2,43857843
Angle of crack 27°	-1	665,23	936,14	-13,918	-57,7472751	-70,5076133	5,62098845	43,3606534	53,9550146	35,3979638	60,8090575
	-0,5	789,93	714,63	-62,773	-51,5466646	-70,4961542	32,4726829	44,8564865	65,8330027	42,1348598	31,1271443
	0	9,15E+02	4,93E+02	-111,63	-41,8030623	-70,5018837	56,708703	39,8772737	62,9550357	28,3316778	28,2487239
	0,5	1039,3	271,62	-160,5	-26,2293902	-69,9570009	155,22302	26,0715153	54,2472231	14,6465895	14,440522
	1	1164	50,115	-209,36	-4,91247141	-70,4285451	-3431,96307	4,91243812	44,3098431	2,46529706	2,40949606
Angle of crack 36°	-1	325,41	1085,3	-20,687	-64,9217133	-70,5081863	5,33699925	28,8197938	??	73,3094742	73,251711
	-0,5	532,5	824,55	-69,395	-58,8332006	-70,4973001	37,2623061	42,3482345	57,1453507	90	
	0	7,40E+02	5,64E+02	-111,89	-48,5992856	-70,4868483	112,778859	43,9580227	61,349608	37,3192801	37,2289802
	0,5	946,69	303,07	-156,14	-30,4932866	-70,4371395	30,1460103	57,1796211	17,7517645	17,686408	
	1	1153,8	42,321	-200,4	-4,19006242	-69,8590251	-89,5897203	4,1900474	43,0006346	2,10064839	2,07026103
Angle of crack 45°	-1	45,415	1127,8	-36,259	-69,7617574	-70,4749547	3,9559238	4,59708842	4,20524134	87,6940214	87,7065617
	-0,5	253,18	853,31	-65,068	-64,9788507	-70,4902426	39,7955485	28,6077951	-52,8930198	73,4741968	73,4153384
	0	5,52E+02	5,79E+02	-113,09	-53,8485442	-70,4772465	40,001056	44,967273	-85,4885887	46,369089	46,2738596
	0,5	850,36	304,28	-155,26	-32,9125391	-70,4348477	-75,7218505	32,3918424	-53,8212114	19,6884752	19,6162528
	1	1148,9	29,761	-200,99	-2,96373523	-69,5708273	-63,0255595	2,96373258	-44,4401734	1,48385277	1,4538401

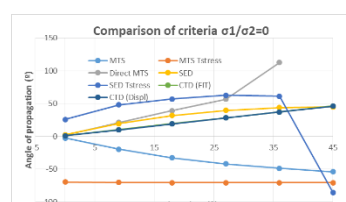
Table 13. Comparison of the angle of propagation for $a/W= 0.4$ for different criteria



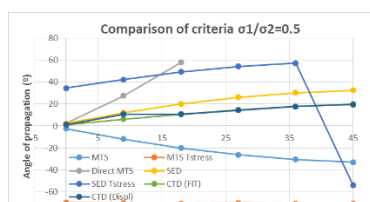
Graph 41.



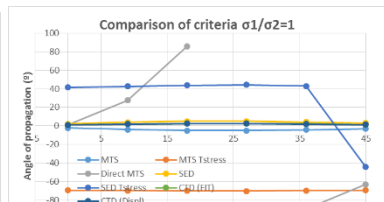
Graph 42.



Graph 43.



Graph 44.

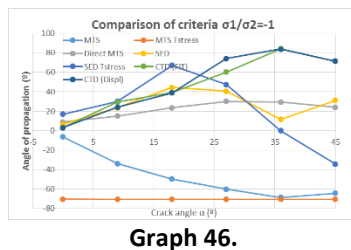


Graph 45.

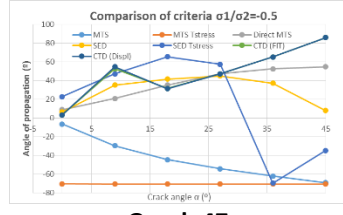
Graph 41, Graph 42, Graph 43, Graph 44, Graph 45. Comparison of the angle of propagation for $a/W= 0.4$ for different criteria

Ratio crack 0,9											
				MTS	MTS Tstress	Direct MTS	SED	SED Tstress	CTD (FIT)	CTD (Displ)	
	σ_1/σ_2	KI	KII	T-STRESS	$\Theta(\text{deg})$						
Angle of crack 0°	-1	3608,2	204,13	-97,356	-6,43514441	-70,4285451	8,91250539	6,43501573	16,9992369	3,23799498	3,21329274
	-0,5	3608,2	204,14	-198,91	-6,43545504	-70,4210967	8,85743653	6,43532633	22,8164774	3,23815327	3,2134555
	0	3,61E+03	2,04E+02	-198,28	-6,43576567	-70,4210967	8,49638034	6,43563693	22,7792351	3,23831156	3,21361991
	0,5	3608,2	204,16	-225,72	-6,4360763	-70,4193778	8,08919095	6,43594753	24,3754955	3,23846984	3,21378309
	1	3608,2	204,17	-152,6	-6,43638693	-70,4245344	7,74798244	6,43625813	20,1207109	3,23862813	3,21394729
Angle of crack 9°	-1	3219,1	1198,6	-117,9	-33,7838566	-70,5110511	14,9385894	33,1850913	57,3692702	20,4223164	20,3210174
	-0,5	3315,4	1021,9	-141,97	-29,6794186	-70,6491339	20,8359127	29,3782758	52,7351875	17,1307772	17,0357282
	0	3,41E+03	8,45E+02	-216,57	-25,1490316	-70,5024567	25,651221	25,0220979	48,261533	13,9126529	13,8255752
	0,5	3508,1	668,35	-267,04	-20,2292576	-70,4944353	31,1130332	20,1878063	43,4441039	10,7865118	10,7073718
	1	3604,4	491,6	-315,31	-15,0008905	-70,4806843	36,630246	14,9918207	8,89073815	7,76658473	7,69482716
Angle of crack 18°	-1	2315,3	1879,1	-166,07	-49,7122757	-70,5167806	23,5871313	44,380363	67,0682997	39,0628217	38,9185595
	-0,5	2573,3	1575,6	-215,22	-44,4125348	-70,5139158	35,146818	41,6904172	65,4187542	31,4786241	31,3537986
	0	2,83E+03	1,27E+03	-243,21	-37,9031793	-70,504781	50,337455	36,7863203	61,307782	24,1967718	24,069956
	0,5	3089,2	968,74	-314,38	-30,0488517	-70,5036026	74,8915936	29,7274458	54,9221674	17,4108655	17,2980618
	1	3347,2	665,3	-386,69	-20,9776782	-70,4909975	137,001066	20,9277627	47,6089341	11,2417754	11,1434351
Angle of crack 27°	-1	1256,7	2204,8	-140,14	-60,1267354	-70,5173536	30,031099	40,709682	47,4542355	60,3175659	74,2485771
	-0,5	1691,8	1831,2	-203,21	-54,3069308	-70,5150618	47,1386466	44,9102938	57,3898966	47,2659288	47,111867
	0	2,13E+03	1,46E+03	-263,44	-46,6190781	-70,5110511	48,1624455	43,0032153	63,8878111	34,4234904	34,2812997
	0,5	2562	1084	-325,83	-36,5890202	-70,5053215	372,344147	35,6680174	60,154991	22,9335595	26,4257533
	1	2997,2	710,41	-406,97	-24,2779167	-70,4921435	-206,691216	24,1721342	51,792099	13,3344293	13,213915
Angle of crack 36°	-1	231,57	2225,2	-98,941	-68,5542183	-70,5190725	29,3477877	11,6348331	??	84,0587833	84,0017248
	-0,5	841,45	1826,9	-175,63	-62,034768	-70,512197	52,5125385	37,2333321	-69,5632268	65,2697237	65,1593535
	0	1,45E+03	1,43E+03	-252,74	-52,8890074	-70,5093322	29,9038184	44,9964718	-83,1194083	44,5503965	44,406551
	0,5	2061,2	1030,4	-314,74	-40,203674	-70,5024567	-123,772047	38,6565533	61,525506	26,5606034	26,4257533
	1	2671,1	632,18	-407,28	-24,2489672	-70,4858409	-63,0908859	24,1438345	52,8027965	13,3154124	13,2055524
Angle of crack 45°	-1	665,8	1993,2	-43,824	-64,2997051	-70,5173536	23,9794547	31,0063195	-34,2495461	71,5288393	71,5225469
	-0,5	114,53	1623,3	-134,06	-69,1871488	-70,4795384	54,8679168	7,99257508	-34,8351089	85,964252	85,9120834
	0	8,95E+02	1,25E+03	-218,17	-57,6917302	-70,5036026	-292,848345	43,4045484	-86,9983325	54,4749074	54,3431318
	0,5	1675,2	883,41	-290,74	-41,337676	-70,4967271	-52,3022058	39,5296885	61,2063685	27,8047431	27,668684
	1	2455,5	513,47	-389,63	-21,8981271	-70,4755277	-28,3104168	21,8359236	51,7302195	11,8109398	11,7040508

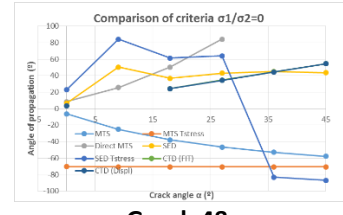
Table 14. Comparison of the angle of propagation for $a/W= 0.9$ for different criteria



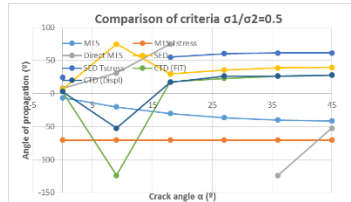
Graph 46.



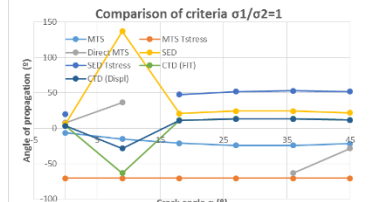
Graph 47.



Graph 48.



Graph 49.



Graph 50.

Graph 46, Graph 47, Graph 48, Graph 49 and Graph 50. Comparison of the angle of propagation for $a/W= 0.9$ for different criteria

7 Conclusion

There is no definitive conclusion as to which method is the best or most accurate for predict the crack propagation angle in nonlinear materials. It can be observed in the previous graphs the deviations of several values that cause the peaks in the graphs.

For small ratios that resemble an infinite plate situation ($a/W = 0.1$) the comparison of results for different criteria are coherent except some values when T-stress is add on the criteria.

The situation for ratio $a/W = 0.9$ it seems to be more complex especially on Direct MTS and on criteria with T-stress.

It would be necessary to do a more in-depth analysis of these results as well as the procedures used and the theory on which it was based to arrive at a firm conclusion. An experimental analysis would be helpful in delimiting the results.

The MTS with T-stress shows for all geometry almost constant angle around 70.5° from $a/W > 0.2$. It can be seen that the length ratio a/W , has an influence on it as well. Also, we it can be surely said that T-stress parameter has a big influence on the value of angle.

8 Author's own work

Miarka, P., Oliver, C., Seitl, S., 2017. Crack initiation angle in the biaxial stress field. 19th Conference Applied Mechanics 2017 – conference proceedings, 2017, pp 69-73.

9 References

1. XIAN-FANG LI , KANG YONG LEE, GUO-JIN TANG. Kink angle and fracture load for an angled crack subjected to far-field compressive loading.
2. AI KAH SOH *, LI CHUN BIAN. Mixed mode fatigue crack growth criteria. (23 November 2000)
3. L. MALÍKOVÁ, V. VESELY', S. SEITL. Crack propagation direction in a mixed mode geometry estimated via multi-parameter fracture criteria. (2011)
4. DANIEL F. C. PEIXOTO A,B*, Paulo M.S.T. de Castro. Mixed mode fatigue crack propagation in a railway wheel steel.
5. J. QIAN and A. FATEMIT. Mixed mode fatigue crack growth: A literature survey (Year...)
6. FRANCISCO JAVIER BELZUNCE VARELA, book of notes subject Technology Of Materials used in Universidad de Oviedo (Escuela Politécnica de Ingeniería) - 2014
7. ANDERSON, Ph.D. Fracture Mechanics. Fundamentals and applications. Third edition CRC-Press (2005)
8. ANSYS Help Viewer
9. MALÍKOVÁ, L., VESELÝ. V., SEITL S., Estimation of the crack propagation direction in a mixed-mode geometry via mlti-parameter fracture criteria.
10. WILLIAMS, M. L., On the stress distribution at the base of a stationary crack. ASME Journal of Applied Mechanics, 1957. 24. 109-114.
11. ERDOGAN, F. AND SIH, G. C., On the crack extension in plates under plane loading and transverse shear. J. bas. Engng, ASME Trans., 1963, 85, 519-525.
12. MATVIENKO, YU. G. Maximum average tangential stress criterion for prediction of the crack path
13. SIH, G. C., Mechanics of Fracture Initiation and Propagation. Kluwer, The Netherlands, 1991
14. JORGE BEDOLLA HERNÁNDEZ. Estimación de Factores de Intensidad de Esfuerzos en Sistemas Mecanismos con Fricción. (2014)
15. JORGE LUIS GONZÁLEZ VELÁZQUEZ. Mecánica de fractura (2004)
16. VÍCTOR ÓSCAR GARCÍA ALVAREZ. Estudio de la fractura en modo mixto de los materiales cuasifrágiles. Aplicación al hormigón. (1997)
17. L. MALÍKOVÁ, V. VESELÝ. Significance of higher-order terms of the Williams expansion for plastic zone extent estimation demonstrated on a mixed-mode geometry.
18. L. MALÍKOVÁ and V. VESELÝ. The influence of higher order terms of Williams series on a more accurate description of stress fields around the crack tip. (27 June 2014) Faculty of Civil Engineering, Institute of Structural Mechanics, Brno University of Technology
19. J. SLADEK, V. SLADEK, P. JEDELINSKI. Contour integrals for mixed-mode crack analysis: effect of nonsingular terms Theoretical and Applied Fracture Mechanics 27 (1997) 115-127
20. M.R. AYATOLLAHI,M.J. PAVIER and D.J. SMITH. Determination of T-stress from finite element analysis for mode I and mixed mode I-II loading. (21 July 1998) *Department of Mechanical Engineering, University of Bristol, Bristol BS8 1TR, UK*



21. M.R. AYATOLLAHI_, M.R.M. ALIHA Fracture toughness study for a brittle rock subjected to mixed mode I-II loading (2006) Iran University of Science and Technology.

22. M.E. KIPP, G.C. SIH, The strain energy density failure criterion applied to notched elastic solids, Int. J.solids Struct. II (1975) 153-173. Lehigh University.

23. DAREN PENG, RHYS JONES. Finite Element Method Study on the Squats Growth Simulation

10 Curriculum vitae

Claudia Oliver Figueira

+34 669 31 71 52

claudia.ofem@gmail.com

31/08/1993



Education	<p>Now studying Bachelor's Degree in Mechanical Engineering (2011- Expected end date May 2017) University of Oviedo – Gijón Polytechnic School of Engineering Erasmus mobility in Brno University of Technology (2017)</p>
Work experience	<p>Internship in CELESTINO RODRÍGUEZ SL. July 2016</p> <ul style="list-style-type: none"> ● Review of documentation of a project for the design of a vacuum drying machine. (Technical specification of the companies, revision of plans, revision of certificates of materials.) ● Participation in a project to adapt the existing machine to another company with different conditions. Analysis and comparative of the different companies that will house the machine for the adaptation process. Analysis of new facilities (dimensions, supplies, available space, electrical connections etc.)
Conferences and articles	<p>Participation in 19th International Scientific Conference APPLIED MECHANICS 2017 Brno, April 25-28, 2017, CZECH REPUBLIC</p> <ul style="list-style-type: none"> ● Crack Initiation angle in the biaxial field. PETR MIARKA, CLAUDIA OLIVER, STANISLAV SEILT. (2017)
Languages	<p>Spanish: Native</p> <p>English: High level. First Certificate in English (B2). August 2016</p>
IT skills	<p>High level in Office. User level in Autocad (2D desing) User level in ANSYS Mechanical APDL User level in Autodesk Inventor (3D desing)</p>
Others	<p>Good communication skills in both, Spanish and English. Ability to work effectively as a part of a team or individually. Travelling and moving disposition. Driving skills (B)</p>